
A THREE-GROUPS NON-LOCAL MODEL FOR COMBINING HETEROGENEOUS DATA SOURCES TO IDENTIFY GENES ASSOCIATED WITH PARKINSON'S DISEASE

A PREPRINT

 **Troy P. Wixson**

Department of Statistics, Colorado State University, Fort Collins CO, USA
twixson@rams.colostate.edu

 **Benjamin A. Shaby**

Department of Statistics, Colorado State University, Fort Collins CO, USA

 **Daisy L. Philtron**

Department of Applied Mathematics and Statistics, Colorado School of Mines, Golden, Colorado, U.S.A.

International Parkinson Disease Genomics Consortium

 **Leandro A. Lima**

Center for Systems and Therapeutics, Gladstone Institute, San Francisco, CA, USA

 **Stacia K. Wyman**

Innovative Genomics Institute, University of California Berkeley, Berkeley, California, U.S.A.

 **Julia A. Kaye**

Center for Systems and Therapeutics, Gladstone Institute, San Francisco, CA, USA

 **Steven Finkbeiner**

Center for Systems and Therapeutics, Gladstone Institutes, San Francisco, CA, USA
Taube/Koret Center for Neurodegenerative Disease, Gladstone Institutes, San Francisco, CA, USA
Department of Neurology and Physiology, University of California San Francisco, San Francisco, California, U.S.A.

June 11, 2024

ABSTRACT

We seek to identify genes involved in Parkinson's Disease (PD) by combining information across different experiment types. Each experiment, taken individually, may contain too little information to distinguish some important genes from incidental ones. However, when experiments are combined using the proposed statistical framework, additional power emerges. The fundamental building block of the family of statistical models that we propose is a hierarchical three-group mixture of distributions. Each gene is modeled probabilistically as belonging to either a null group that is unassociated with PD, a deleterious group, or a beneficial group. This three-group formalism has two key features. By apportioning prior probability of group assignments with a Dirichlet distribution, the resultant posterior group probabilities automatically account for the multiplicity inherent in analyzing many genes simultaneously. By building models for experimental outcomes conditionally on the group labels, any number of data modalities may be combined in a single

coherent probability model, allowing information sharing across experiment types. These two features result in parsimonious inference with few false positives, while simultaneously enhancing power to detect signals. Simulations show that our three-groups approach performs at least as well as commonly-used tools for GWAS and RNA-seq, and in some cases it performs better. We apply our proposed approach to publicly-available GWAS and RNA-seq datasets, discovering novel genes that are potential therapeutic targets.

Keywords First keyword · Second keyword · More

1 Introduction

A substantial portion of the risk of developing even so-called “sporadic disease” is attributable to genetic variants harbored by an individual. For this reason, huge genetic studies have investigated many major human diseases to uncover genetic variants that either directly cause or modify disease, first with the analysis of single nucleotide variants (SNVs), then whole exomes, and now, increasingly, whole genomes. Conventionally, the analysis of genomic data focused on genome-wide association studies (GWAS), which have been used to identify associations in a gene variant and disease incidence or progression to determine if a genetic variant is correlated with a disease phenotype (Uffelmann et al., 2021). This is typically accomplished by performing a simple statistical test for association between a particular genetic variant and a disease, adjusting for multiple comparisons made across the genome. However, the variants identified in this way from GWAS studies of complex traits, such as human disease, usually explain only a small fraction of the known heritability, and the effect sizes of the variants themselves are typically small. Some of the missing heritability appears to arise from common variants whose effect sizes are too small to detect using GWAS, even when the sample size is large (Boyle et al., 2017).

Transforming genetic discoveries into advances in our understanding of pathogenesis and new treatments is a major unmet need. Whereas rare Mendelian diseases typically arise from mutations in specific genes, the risk of developing common diseases is believed to be a complex trait conferred by the cumulative effect of multiple genetic variants. Critically, the experiments required to functionally validate the role of a specific variant are resource intensive, and the number of potentially important variants that emerge from genetic studies vastly exceeds the capacity and resources available to evaluate them.

This paper details an approach to begin to meet this need by integrating data sources across multiple experimental types to reliably detect weak genetic signals related to PD. The approach outlined here detects genes associated with PD by probabilistically classifying genes as belonging to a null group, a deleterious group, or a beneficial group using joint models of the relationship of disparate data types to disease status. In this framework genes in the null group are unassociated with the disease, genes in the beneficial group are associated with either a better outcome or decreased incidence of a negative outcome, and genes in the deleterious group are associated with a worse outcome or increased incidence of a negative outcome. The data types we will consider are GWAS data and RNA-seq data, although, importantly, the modeling framework is completely modular, so that additional data types can easily be added when they become available. It also does not require the data types to be observed on a common set of individuals. Each data type has its own sub-model, specified conditional on the set of gene labels (i.e. null, beneficial, or deleterious). In the GWAS branch, the response is disease status (i.e. binary presence or absence), and in the RNA-seq branch the response is expression level (i.e. counts).

The statistical framework we propose enhances the power to detect weak signals by borrowing strength across different sources of information. This approach differs in important ways from established methods in the literature. The combination of multiple datasets or studies has historically used meta-analysis, which collects the results of several analyses that have been performed separately and combines them *post hoc*. A critical weakness of meta-analysis is that the analysis of each individual dataset is siloed and, therefore, information cannot be shared among datasets. Subsequent combination of individual results tries to take advantage of the accumulation of evidence but cannot not take advantage of the statistical benefits of borrowing strength.

Traditional meta-analysis approaches for integrating data sources perform separate analyses for each data type and then combine the resulting p -values. Many techniques for p -value combination exist, including Fisher’s or Stouffer’s techniques (Fisher, 1929; Stouffer et al., 1949) as well as more modern approaches (Genovese and Wasserman, 2004; Benjamini and Heller, 2008). In contrast, our proposed approach shares information across all data types simultaneously to inform the analysis, increasing power to detect weak signals and providing the ability to handle information that may be missing or unreliable in any single data type.

Several previous studies have also emphasized the benefits of analyzing different datasets jointly, a strategy sometimes referred to as meta-dimensional methods (Ritchie et al., 2015) or multi-modal analysis (see Richardson et al., 2016; Li

et al., 2018, for reviews). However, previous approaches to integrating multiple genomic data types are not directly applicable to our PD analysis, as they require either the same subjects in each experiment type, the same experiment types, or *a priori* grouping of genes into sets (see, e.g. Ding et al., 2022; Holzinger et al., 2013; Tyekucheva et al., 2011, and references therein).

Our proposed model-based three-groups framework has two key features. First, by apportioning prior probability of group assignments with Dirichlet distributions, the resultant posterior group probabilities automatically account for the multiplicity inherent in analyzing many genes simultaneously (Scott and Berger, 2010). Second, by building models for experimental outcomes conditionally on the group labels, any number of data modalities may be combined in a single coherent probability model, allowing information sharing across experiment types. These two features result in parsimonious inference with few false positives, while simultaneously enhancing power to detect signals.

Importantly, the hierarchical three-groups structure is completely modular; as long as a collection of experimental outcomes can be formalized conditionally upon latent group labels, any collection of them can be easily combined. This flexibility is achieved by modeling the response for each experimental data type as being conditionally independent given the collection group labels for each gene. Letting $\mathbf{Y}_1, \dots, \mathbf{Y}_M$ be response vectors for M experimental data types, $\theta = (\theta_1^T, \dots, \theta_M^T)^T$ the model parameters corresponding to sub-models for the M experimental types, and \mathbf{G} the group labels (which are shared across all response types), conditional independence allows the full data likelihood to be factorized as

$$\mathcal{L}(\mathbf{Y}_1, \dots, \mathbf{Y}_M | \mathbf{G}, \theta) = \prod_{m=1}^M \mathcal{L}_m(\mathbf{Y}_m | \mathbf{G}, \theta_m).$$

In the present study, we consider a pair of experiments: an RNA-seq study in which biological samples of PD and control patients are assayed for differential expression, and a GWAS study where PD and control populations with no familial relationships are genotyped (Nalls et al., 2014). The model for the outcome of these two experiments is specified separately, with the exception of the group labels of each gene, which are shared across both experiments. In each model, the effect of each gene is expressed conditionally on its unknown group assignment.

An additional benefit of this hierarchical three-groups structure is that, like many hierarchical Bayesian formulations, it straightforwardly accommodates the common situation where some genes are not measured in all data types. Genes that are included in some, but not all, experiment types are simply treated as missing data by iterative sampling from their posterior predictive distributions in the experiments from which they are absent. This flexibility is not available, for example, to p -value combination approaches which require genes to be measured in all data types.

Ultimately, scientific interest lies mostly in the posterior probabilities of the group assignments. Genes with high posterior probability of being either beneficial or deleterious will be considered targets for our follow-up experiments, potentially as therapeutic targets.

2 Model Details

The proposed three-groups suite of statistical models requires the separate development of a model for each experimental data type, conditional on the collection of genes belonging to null, deleterious, or beneficial groups. Each sub-model is tailored to its particular response type, but each is built upon the common three-groups structure, allowing pooling of information through the shared group labels.

2.1 A Three-component Mixture and Automatic Multiplicity Adjustment

Models for GWAS data with binary responses and for RNA-seq data with count responses, as well as any future data types, are constructed around a core three-component mixture distribution. The unknown group label G_j for gene j has a categorical distribution with probability vector denoted as $\lambda = (\lambda_1, \lambda_2, \lambda_3)^T$, exchangeably across all genes $1, \dots, J$. The common structure across the sub-models induces sharing of information among the disparate data types. In addition, placing a prior distribution on λ results in a penalty for large numbers of non-null genes that acts as an automatic adjustment for multiple comparisons, and hence results in few false positives. This automatic adjustment is an alternative to the common practice of performing many independent tests and adjusting p -values *post hoc* (Benjamini and Hochberg, 1995, e.g.).

The apportionment of prior mass on λ depends on the number of comparisons J and induces automatic multiplicity adjustment (Scott and Berger, 2010). Let $\mathcal{M}_{\mathbf{G}}$ be the model with group assignments \mathbf{G} , and assign the hyper-prior distribution $\lambda \sim \text{Dirichlet}(\kappa \mathbf{a})$. Define $(k_1, k_2, k_3)^T$ as the number of genes in groups 1, 2, and 3 as determined by \mathbf{G} (so that $k_1 + k_2 + k_3 = J$). Then the prior probability mass function (pmf) for each model $\mathcal{M}_{\mathbf{G}}$ given λ is

$P(\mathcal{M}_{\mathbf{G}} | \lambda) = \binom{J}{k_1, k_2, k_3} \lambda_1^{J-k_2-k_3} \lambda_2^{k_2} \lambda_3^{k_3}$ and the marginal prior pmf for each model $\mathcal{M}_{\mathbf{G}}$ is

$$p(\mathcal{M}_{\mathbf{G}}) = \int_{\lambda} P(\mathcal{M}_{\mathbf{G}} | \lambda) \pi(\lambda) d\lambda = \frac{\Gamma\left(\sum_{i=1}^3 \kappa a_i\right) \prod_{i=1}^3 \Gamma(\kappa a_i + k_i)}{\prod_{i=1}^3 \Gamma(\kappa a_i) \Gamma\left(\sum_{i=1}^3 \kappa a_i + k_i\right)}.$$

For simplicity of visualization, assume that $k_2 = k_3$, so that $k_2 + k_3$ is the number of non-null genes, and $k_1 = J - k_2 - k_3$. Also assume for simplicity that $\kappa = 1$ and $\mathbf{a} = (1, 1, 1)^T$. If $J = 1,000$, then the log marginal prior pmf for each model $\mathcal{M}_{\mathbf{G}}$, as a function of the number k of non-null genes is displayed in Figure 1.

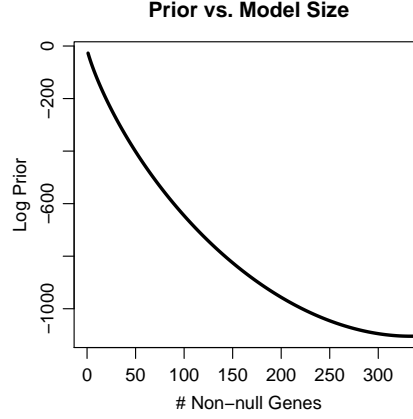


Figure 1: The log prior probability mass function for models $\mathcal{M}_{\mathbf{G}}$ corresponding to group assignments \mathbf{G} , as a function of the number of non-null elements in \mathbf{G} . The penalty for including more non-null genes in the model is strong, resulting in an aggressive multiple comparisons adjustment.

Figure 1 shows a strong prior preference for models with few genes classified as non-null. In this example with $J = 1,000$ candidate genes, models with 50 non-null genes are many thousands of times less likely *a priori* than models with no non-null genes. This strong prior preference depends on J and results in posterior inference with few false positive genes.

2.2 Three-Groups Model for RNA-seq Data

RNA-seq expression levels are measured as counts, necessitating statistical approaches that either model the data using discrete distributions such as Poisson or Negative Binomial (e.g., edgeR (Robinson et al., 2010) and DESeq2 (Love et al., 2014)) or normalize the data before applying statistical models that were designed for continuous responses (e.g., limma+voom (Law et al., 2014)). In either case, the goal of analysis is to discover genes that are differentially expressed between the treatment (disease) and control (healthy) groups.

Let $Y_{ijk}^{\text{RNA-seq}}$ be the count for the i^{th} replicate of the j^{th} gene for treatment group $k \in \{0, 1\}$. Similarly to edgeR we model $Y_{ijk}^{\text{RNA-seq}}$ using the Negative Binomial distribution, using a mean and dispersion parametrization: $Y_{ijk}^{\text{RNA-seq}} \sim \text{NegBin}(\mu_{ijk}, \phi_j)$, where μ_{ijk} is the mean count from individual i of gene j from treatment group k , and ϕ_j is the dispersion parameter for gene j . The variance of Y_{ijk} is then $\mu_{ijk}(1 + \mu_{ijk}\phi_j)$. We model the mean counts as

$$\log(\mu_{ijk}) = \alpha_j + \log(fc)_j * k + L_i + M_j + (\mathbf{X}_i^{\text{RNA-seq}})^T \beta^{\text{RNA-seq}}.$$

Here α_j is the gene-wise intercept, $(fc)_j$ is the fold change between expected counts in the treatment group compared to the control group, L_i and M_j are known offsets that are equal to the natural logarithm of the library size for sample i and the gene length for gene j respectively, and $(\mathbf{X}_i^{\text{RNA-seq}})^T$ is a row-vector of covariates associated with individual i from the RNA-seq study. Expected counts are proportional to both library size and gene length and thus they are included directly within the Negative Binomial model as offsets, as an alternative to normalizing the data as a pre-processing step, which is common in standard analysis tools (Robinson et al., 2010; Love et al., 2014; Law et al., 2014).

The fold change $(fc)_j$ of the counts associated with each gene is the focus of the inference, and hence is endowed with the three-groups structure:

$$\log(fc)_j \sim \begin{cases} 0 & \text{if } G_j = 1 \text{ (Null)} \\ f^{\text{RNA-seq}^+} & \text{if } G_j = 2 \text{ (Deleterious)} \\ f^{\text{RNA-seq}^-} & \text{if } G_j = 3 \text{ (Beneficial)} \end{cases} \quad (1)$$

where $f^{\text{RNA-seq}^+}$ is a distribution over the positive half-line and $f^{\text{RNA-seq}^-}$ is a distribution over the negative half-line (see Section 2.4).

We induce shrinkage on the gene-wise dispersion using a shared random effect scheme:

$$\begin{aligned} \log(\phi_j) &\sim \text{N}(\mu_0, \text{precision} = \tau_0) \\ \mu_0 &\sim \text{N}(0, \text{precision} = 10^{-2}) \\ \tau_0 &\sim \text{t}^+(\nu = 4), \end{aligned}$$

To complete the model, we assign the vague priors $\alpha_j \sim \text{N}(0, \text{precision} = 10^{-3})$ and $\beta_l^{\text{RNA-seq}} \sim \text{N}(0, \text{precision} = 10^{-3})$, independently for $j = 1, \dots, J$ and $l = 1, \dots, L^{\text{RNA-seq}}$, where $L^{\text{RNA-seq}}$ is the number of covariates considered.

2.3 Three-Groups Model for GWAS Data with Binary Outcomes

GWAS entails collecting genotypic (i.e. SNVs) and phenotypic data from unrelated individuals with the goal of associating specific SNVs with disease outcomes. A complication arises in that our model formulation for the RNA-seq data type, the unit of measurement is the gene; however, GWAS data are collected on the SNV level. Thus, integrating GWAS with the other models requires that SNVs be either summarized into their associated genes or identified as non-coding variants with no obvious parallel in our RNA-seq dataset. The need to aggregate SNV information to the gene level is not unique to our formulation and is also necessary, for example, for burden tests for association (Asimit et al., 2012; Morgenthaler and Thilly, 2007; Li and Leal, 2008; Madsen and Browning, 2009). How best to formalize the association between SNVs and genes is an open question (see, e.g., Gazal et al., 2022 and references therein). The simplest approach, which we take here, is to collapse SNVs into genes in a binary fashion: if a gene contains a SNV in or near its coding region, it is assigned a value of 1, if it does not contain a SNV, it is assigned a value of 0. In this binary collapse we assume a dominant model of disease (i.e., having one or more copies of the associated minor allele alters the risk). A simple alternative strategy is to sum the number of minor alleles in or near each gene’s coding region. Extensions include using weighted sums, and schemes allowing for different SNVs in a single region to act in opposite ways on the outcome.

Our three-groups model for GWAS is logistic regression, as the response is binary (1 if individual i in the GWAS study has PD and 0 otherwise). The response Y_i^{GWAS} is modeled as a Bernoulli random variable with probability p_i of being in the PD group, with

$$\text{logit}(p_i) = \mathbf{z}_i^T \boldsymbol{\gamma} + (\mathbf{X}_i^{\text{GWAS}})^T \boldsymbol{\beta}^{\text{GWAS}},$$

where $\mathbf{z}_i^T \boldsymbol{\gamma}$ are gene effects and $(\mathbf{X}_i^{\text{GWAS}})^T \boldsymbol{\beta}^{\text{GWAS}}$ are individual-level covariate effects. The gene effects are the focus of the inference, and thus the $\boldsymbol{\gamma}_j$ s are endowed with a three-groups prior structure analogous to (1) from Section 2.2. The vague prior $\beta_l^{\text{GWAS}} \sim \text{N}(0, \text{precision} = 10^{-3})$ for the individual level covariates $l = 1, \dots, L^{\text{GWAS}}$ completes the model.

2.4 Gene Effect Priors

Secondary scientific interest, after group assignment probabilities, lies in the magnitude of gene effects. Group assignments are informed by these gene effects, and the effect sizes contain some information regarding the potential benefit of clinical interventions. The three-groups framework allows for flexible modeling of these effect sizes through selection priors which may be asymmetric. That is, a point mass at zero represents the null effect size, and we allow the the distribution of beneficial effect sizes ($f^{(m)-}$) to differ from the distribution of deleterious effect sizes ($f^{(m)+}$). This added flexibility above standard, symmetric, selection priors reflects the biological reality that genes with protective effects may behave very differently than genes with damaging effects.

Discontinuous “spike and slab”-type priors can be broadly categorized as *local* and *non-local* (Johnson and Rossell, 2010). A prior is said to be local if the density for its “slab” component is non-zero in the neighborhood of its null value (i.e., the gene is a null gene). Conversely, a prior is said to be non-local if the density for its “slab” component is exactly zero in the neighborhood of its null value. Intuitively, the benefit of non-local priors is that effects that might

otherwise be estimated to be trivially small get pushed into the null group because very small effects have zero prior probability. In this study, we consider a non-local prior and compare the results to local three-groups model which has half-normal priors for the non-null gene effects (and thus the slab component is symmetric).

The non-local prior that we consider here is a modification of the product inverse moment (piMOM) prior from Johnson and Rossell (2010), defined by the density $f(\beta|\tau, r) = [\tau^{r/2}/\Gamma(r/2)]^J \prod_{j=1}^J |\beta_j|^{-(r+1)} \exp(-\tau/\beta_j^2)$. This is a two-parameter family, with r controlling the tail decay (smaller r gives heavier tails) and τ controlling the scale. To allow for asymmetry in the non-null gene effects, we truncate the density and use the positive component that has support on \mathbb{R}^+ for deleterious effects and, and separately use a negative component that has support on \mathbb{R}^- for the beneficial gene effects. Separate half-piMOM hyper-priors are placed on each of the τ parameters of these truncated densities, which allows us to consider the separate posterior distributions of beneficial and deleterious gene effects. Together with a spike component at zero, we thus arrive at a three-component mixture for the null, beneficial, and deleterious gene effects. Previous work on variable selection tasks using non-local priors (Johnson and Rossell, 2010, 2012; Nikooienejad et al., 2016; Li and Chekouo, 2022, e.g) found improved performance when using non-local priors relative to standard local selection priors. Johnson and Rossell (2012) demonstrated that Bayesian model selection procedures based on the piMOM prior density with $r \geq 2$ results in consistent estimation of the true model. Here, we follow their recommendation and fix the tail decay rate at $r = 2$.

3 Computation

For computational efficiency, we use a stick-breaking representation for the Dirichlet-multinomial portion of the model. That is, for $\lambda \sim \text{Dirichlet}(\kappa\mathbf{a})$ the marginal distribution of each component follows a Beta distribution (e.g. $\lambda_1 \sim \text{Beta}(\kappa a_1, \kappa a_2 + \kappa a_3)$) which allows us to model the prior probabilities according to two Beta distributions: one controlling the prior probability of being a null gene and the other controlling the conditional probability of being beneficial given the gene is not in the null group (Gelman, 2014, pg. 585). Correspondingly, the marginal and conditional distributions of categorical random variables are Bernoulli.

The analysis was performed using reversible jump Markov chain Monte Carlo (RJMCMC) (Green, 1995) which speeds up computation and accounts for the inherent change of dimensionality when group assignment changes. The sampler was implemented within the NIMBLE R package (de Valpine et al., 2017, 2023).

4 Simulations

In this section, we explore the behavior of our three-groups framework with non-local gene effects relative to a local three-groups model which has symmetric gene effects and relative to standard analysis pipelines and combinations thereof. Although we tried to replicate key features of real genomic data in our simulated datasets, in the end the simulated data are illustrative only; thus, the total number of simulated genes is small ($J = 250$) to allow for uncluttered visualizations. In each scenario, we assigned five genes to have beneficial effects and five genes to have deleterious effects, with the remainder being null. Each simulated dataset includes a GWAS dataset and an RNA-seq dataset, which are independent conditional on a shared collection of gene labels. To approximately reflect the sample sizes in our actual datasets, we simulated 1,000 individuals for GWAS and 100 individuals for RNA-seq. For a full description of the simulated data please see the Appendix.

We used each of the 250 simulated sets of joint GWAS and RNA-seq data to compare thirteen different models. These models included conventional, non-local three-groups, and local symmetric three-groups models for GWAS alone (Figure 2), RNA-seq alone (Figure 2(a)), and joint models (Figure 2(b)). In the joint three-groups models, the GWAS and RNA-seq models are combined into a single hierarchical model as described in Section 1. The conventional methods are combined using Fisher’s p -value combination method (Fisher, 1929). We chose competitor models for comparison based on what we take to be the most common analysis pipelines in the literature. Specifically, we used individual logistic regression (i.e. one logistic regression per gene, independently across genes) for GWAS; DESeq2, edgeR, and limma+voom for RNA-seq; and Fisher’s p -value combination of the aforementioned models for joint models. Competitors methods were run with their default settings (including normalization) from the standard packages on Bioconductor.

For the reference methods, we control for multiple comparisons using the local false discovery rate (lFDR) adjustment (Efron et al., 2001). We chose local false discovery rate over similar adjustment methods because its interpretation makes it nearly directly comparable with posterior probabilities that result from Bayesian selection procedures. Specifically, the lFDR can be interpreted as the probability of a gene belonging to the null group conditional on the value of its test statistic (Efron et al., 2001).

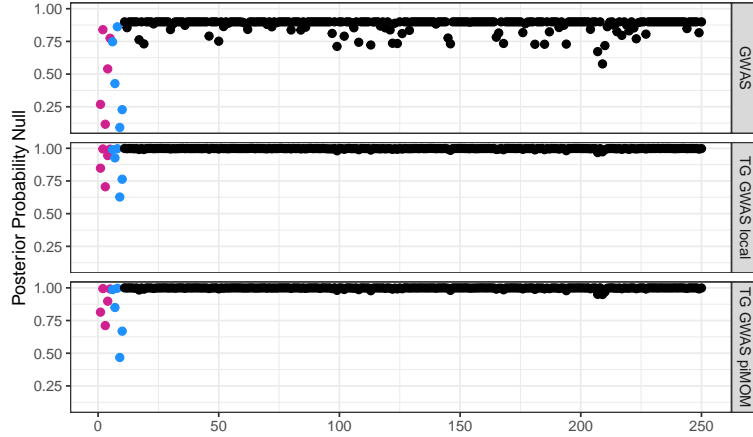


Figure 2: Posterior probability of inclusion in the null group for GWAS only methods, from a single simulated dataset. The top plot shows the individual logistic regression results, the middle plot shows our three-groups GWAS model with local priors on gene effects, and the bottom plot shows our three-groups GWAS model with piMOM priors on gene effects. Genes in blue were simulated to be deleterious, genes in purple were beneficial, and genes in black were null.

As an illustration, Figures 2 and 3 show the posterior probability of inclusion in the null group for each gene, from a single simulated dataset. Each dot represents a gene, and its height represents the posterior probability of being in the null group. The black dots are true null genes, and the colored dots are true non-null genes. The three-groups model further generates posterior probabilities of being in the beneficial and deleterious groups (not shown). Figures 2 and 3 give some idea of how well each of the methods separates null from non-null genes. We investigate this more formally by considering performance across the 250 simulated joint datasets.

We assess the simulations using a variety of performance metrics. Each metric is computed on each model for each simulated dataset, and then the models are compared using boxplots of the aforementioned metrics. This allows us to consider the performance of each model across the many simulated datasets, which aids in understanding variability. First, we consider the log score and Brier score (Gneiting and Raftery, 2007), oriented so that smaller values correspond to better performance (Figure 4). These are both proper scoring rules which have attractive theoretical properties (Gneiting and Raftery, 2007). Both scores reward correct classifications more when they are made with higher confidence, and conversely penalize incorrect classifications more when they are made with higher confidence.

The results in Figure 4 suggest that the three-groups versions of GWAS and RNA-seq, taken separately, are uniformly at least as good as standard analysis tools, and in some cases much better. Particularly striking is how much better the three-groups RNA-seq model performs in terms of log score, relative to DESeq2, edgeR, and limma+voom. This, again, is obtained without any normalizing schemes or elaborate tuning in the three-groups model. The Brier scores show less dramatic differences.

Consideration of Figures 2 and 3 suggests that the choice of cutoff for the classification boundary between null and non-null should vary by model. To assess performance of models at differing cutoffs, we compare the area under the receiver operating characteristic (ROC) curve (Figure 4(c)), a popular metric in the classification literature. In addition, we show as the true positive rate (i.e. power) computed at a cutoff for each model set such that each resulted in a fixed average false positive rate (Figure 4(d)). The joint models are superior to individual models in each metric and our three-groups family of models correctly identifies at least as many non-null genes as competitors while including very few false positives.

These simulations (and others shown in the Appendix) demonstrate the value in the joint structure of our model (even when most of the signal comes from one data type). Finally, a recurring theme in our investigation was the sparsity imposed by the three-groups family of models; Figures 2 and 3 demonstrate that the three-groups models have a strong preference for fewer non-null genes, as explained in 2.1, even with a uniform (i.e. non-informative) prior on the unit simplex for the group inclusion probabilities.

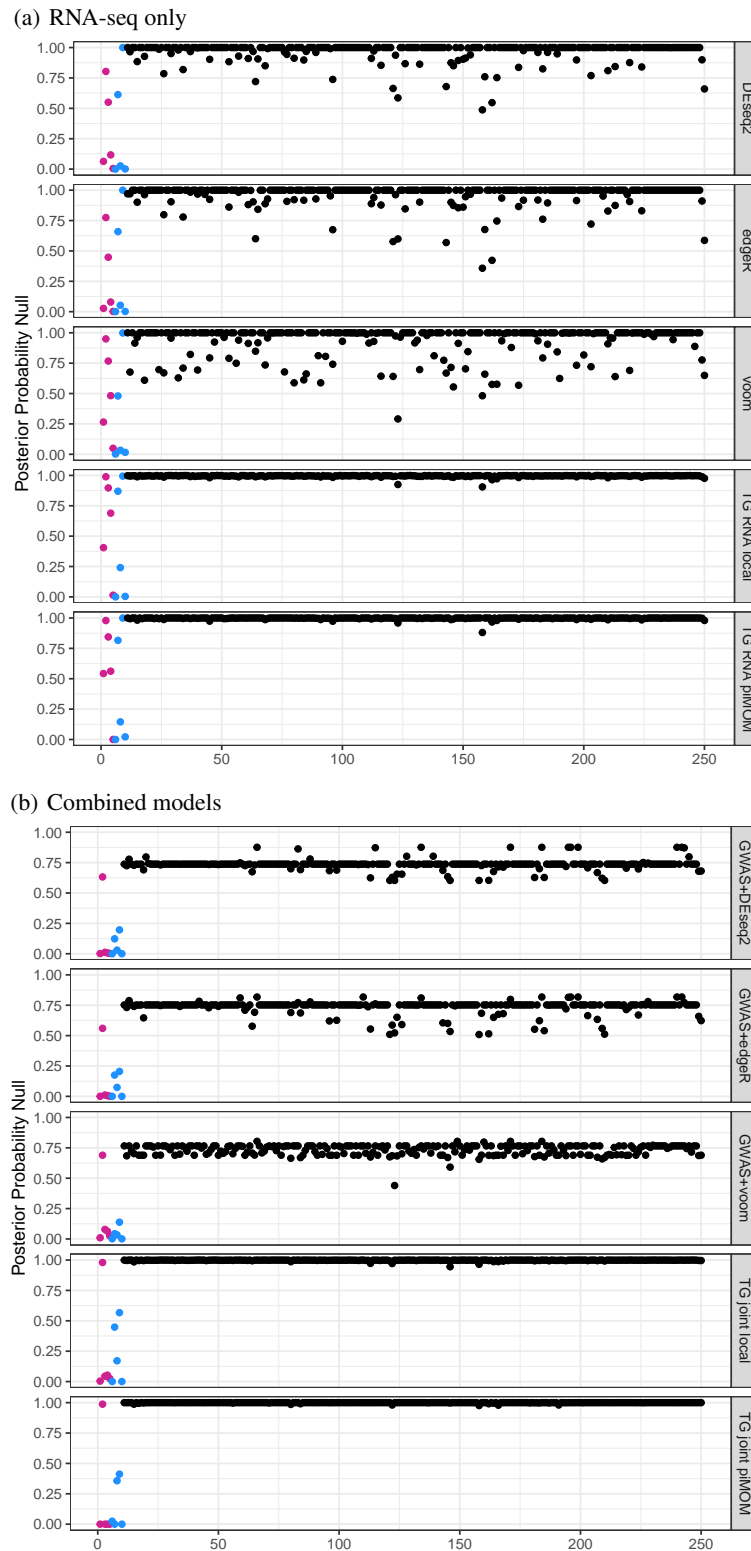


Figure 3: Panel (a) shows posterior probabilities of inclusion in the null group for RNA-seq only methods, from a single simulated dataset. Panel (b) shows the same, but for joint GWAS and RNA-seq methods. The top three plots in each panel are results from standard analysis tools, and the bottom two plots in each panel are results from our local and non-local three-groups models. The color scheme is the same as in Figure 2.

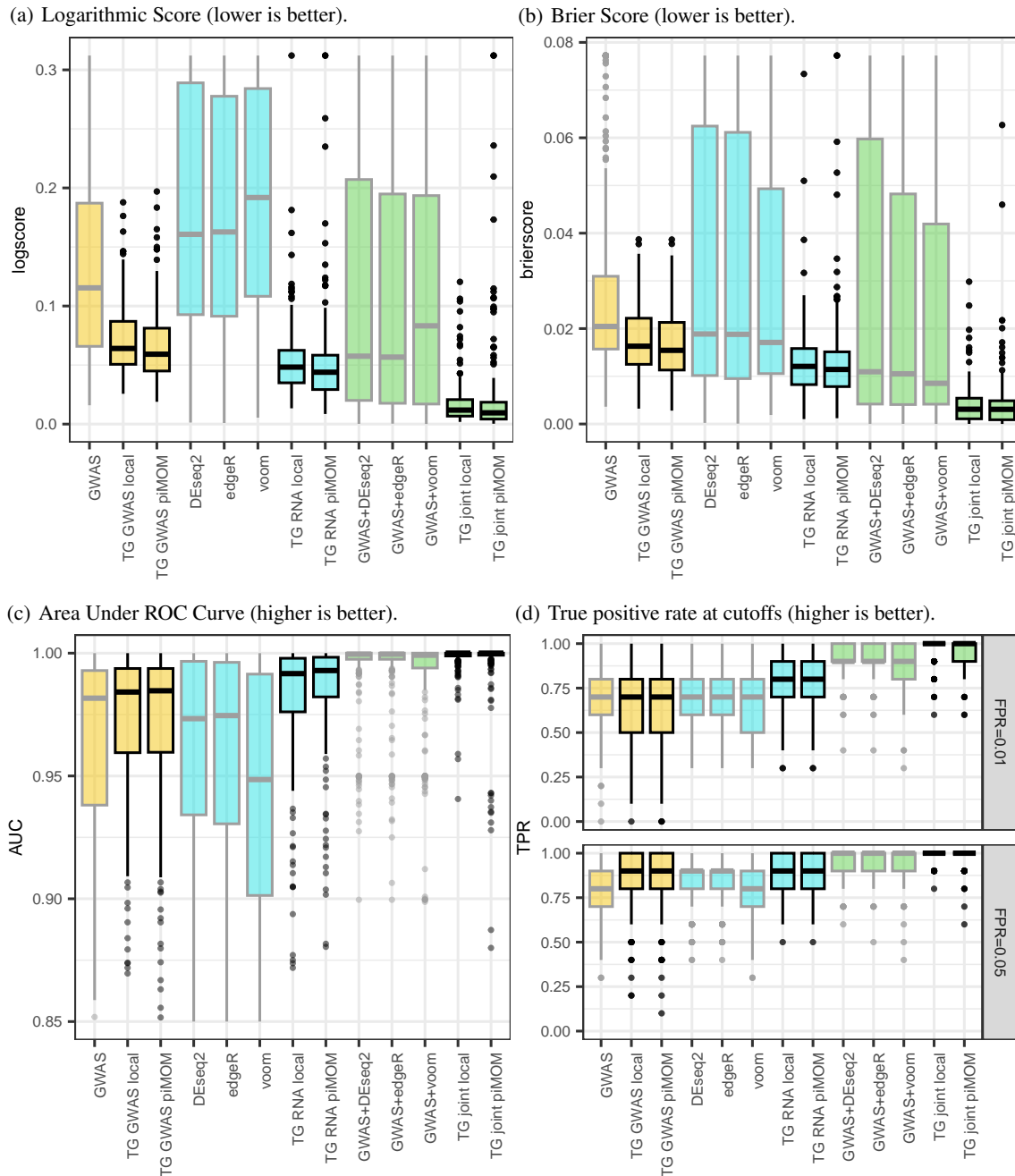


Figure 4: Boxplots of logarithmic scores (a), Brier scores (b), area under receiver operating characteristic curve (c) computed from posterior probability of inclusion in the null group, and the true positive rates (i.e. power) computed at classification cutoffs that result in mean false positive rates of 0.01 (top panel) and 0.05 (bottom panel) in (d) for each of 13 different models, based on 250 simulated datasets. Yellow indicates GWAS only models, blue indicates RNA-seq only models, and green indicates joint models. Boxplots for our three-groups models have black lines, while competitors have grey lines. Panels (a), (b), and (c) show Winsorized boxplots to focus on the bulk of the distribution of points.

5 Parkinson’s Disease Analysis

5.1 Description of the Data

The data that we used for the GWAS branch of this study came from the International Parkinson’s Disease Genomics Consortium (IPDGC) NeuroX Dataset (Nalls et al., 2014). Due to the intense computational burden of running the full MCMC, we analyzed a subset of the full genome. We chose the 2,000 genes that exhibited the largest differential expression between the cortex and the substantia nigra (the region most affected in PD) in Agarwal et al. (2020), as well as 19 additional genes which seemed promising in exploratory analyses. We associated each allele with a particular gene if it was annotated within that gene in the GWAS data (including intronic and 5’ or 3’ UTR plus 3kbp). This resulted in a list of 53,559 variants associated with the 2,019 genes. The NeuroX dataset included 1,734 of the 2,019 genes on our list, sequenced from 11,402 individuals. We then summarized the SNV data to the gene level using an indicator function for whether a given gene was mapped to at least one SNV. In our analysis, we also included the subject-specific covariates age and sex from the NeuroX dataset, and used PD status as the response for all individuals.

The RNA-seq data that we used came from the Parkinson’s Progression Markers Initiative (PPMI), obtained from PPMI upon request. We selected data from the individuals who were identified as healthy controls or untreated PD cases, resulting in data for 370 individuals. We again extracted data from genes that appeared in the same list of 2,019 genes, resulting in data on 1,697 genes (37 genes only had data in the NeuroX dataset). In addition to RNA fragment counts for each individual, we included age, years of education, race, sex, and the phase of the PPMI study as covariates.

5.2 Description of the Analysis

We performed six separate analyses on the aforementioned data. The six models consisted of symmetric local and asymmetric non-local versions of each of: the full joint three-groups GWAS and RNA-seq model, the GWAS branch of the three-groups model by itself, and the RNA-seq branch of the three-groups model by itself. These six models allow for comparisons between our joint and individual models, as well as comparisons between the local and non-local versions of the models. In each case, we ran the MCMC for 20,000 iterations and threw out the first 10,000 as burn-in, as indicated by trace plots. Based on the simulations, we expect genes with strong signal in one sub-model or weak signal in both sub-models to retain signal in the joint model. Conversely, we expect genes with weak signal in only one sub-model to have very weak signal in the joint model, when the weak signal in one branch is not strong enough to overcome the multiplicity penalty induced by the prior.

5.3 Results

One of the benefits of the three-groups family of models is the sparsity it induces due to the built-in multiplicity adjustment, in addition to the borrowing of strength across both genes and sub-models. This induced sparsity is evident in this analysis: more than 1,650 of the 1,734 genes in the full analysis have posterior probability of being null which is greater than 0.99. We expect that, operationally, the x genes with the smallest posterior probability of being null will be investigated further in mouse models or human iPSC cell models by knocking down the genes using siRNA or CRISPRi/a etc., where x is determined by available resources such as budget and personnel time. We report genes as deleterious or beneficial according to the so-called median probability model (inclusion cutoff of 0.5, hereafter MM, (Barbieri and Berger, 2004)), according to their posterior group labels. For comparisons to standard GWAS and RNA-seq analysis tools, the MM cutoff applied to IFDR-adjusted p -values does not produce useful results; the MM for GWAS combined with edgeR, limma+voom, and DESeq2 results in the inclusion of 418, 220, and 533 genes respectively. For these methods, we instead use a more conventional cutoff of 0.05, which results in a comparable number of “interesting” genes as the three-groups family of models under the MM criterion (14, 8, and 27, respectively, compared to 7 and 21 under the local and non-local versions of the three-groups joint model).

The MM for the GWAS only and RNA-seq only local sub-models included 440 and 10 genes, respectively. The joint local MM, by contrast, included just 7 non-null genes. The borrowing of strength appears to have played a larger role in the non-local case; the GWAS only and RNA-seq only non-local sub-models under the MM criterion included 22 and 3 genes, respectively, whereas the joint non-local MM included 21 genes. Two of the genes identified in the GWAS only non-local MM and one of the genes identified in the RNA-seq only non-local MM are included in the joint non-local MM.

The joint three-groups model with local priors identifies three beneficial and four deleterious genes. The three beneficial genes are *CDIP1*, *CHCHD6*, and *CNTNAP2*. These genes are known to be involved in dysregulated pathways in PD; mitochondrial function (Bose and Beal, 2019; Zaltieri et al., 2015), synaptic function (Clayton and George, 1998; Morais et al., 2009), and apoptosis (Tatton et al., 2003; Mochizuki et al., 1996). The four deleterious genes are *DUSP1*, *FAM49B*, *IFRD1*, and *SYTL3* also all have functions in previously implicated PD pathways such as

Table 1: Genes identified as non-null in at least one of the three-groups models. A gene is classified as non-null in all models with an “×”. P_{null} , $P_{\text{ben.}}$, and $P_{\text{del.}}$ are the proportion of the 10,000 mcmc iterations that the gene was in the null, beneficial, and deleterious group respectively. Effect sizes are computed conditionally (i.e., the mean of the effect size when the gene was non-null). GWAS effect sizes are odds ratios; a value less than 1 represents a protective effect and a value greater than 1 represents a damaging effect. RNAseq effect sizes are fold changes and are interpreted similarly. Gene effects with “*” indicate that the gene was null $> 99\%$ of the MCMC iterations in that model.

Gene	local	piMOM	GWAS + edger	GWAS + limma	GWAS + DESeq2	P_{null} local	$P_{\text{ben.}}$ local	$P_{\text{del.}}$ local	P_{null} piMOM	$P_{\text{ben.}}$ piMOM	$P_{\text{del.}}$ piMOM	GWAS effect local	RNA effect local	Disp. local	GWAS effect piMOM	RNA effect piMOM	Disp. piMOM
1 CDIP1	x	x	x	x	x	0.26	0.65	0.09	0.49	0.38	0.13	0.36	0.93	0.14	0.41	0.87	0.14
2 CHCHD6	x	x	x	x	x	0.00	1.00	0.00	0.00	1.00	0.00	0.81	0.9	0.16	0.8	0.86	0.16
3 DUSP1	x	x	x	x	x	0.00	0.00	1.00	0.00	0.00	1.00	1.12	1.19	0.09	1.24	1.19	0.09
4 CNTNAP2	x	x	x			0.00	1.00	0.00	0.00	1.00	0.00	0.67	0.48	1.17	0.71	0.51	1.16
5 SYTL3	x	x	x		x	0.16	0.08	0.76	1.00	0.00	0.00	1.14	1.11	0.08	*	*	0.08
6 FAM49B	x	x				0.00	0.00	1.00	0.00	0.00	1.00	2.19	1.06	0.02	8.67	1.09	0.02
7 IFRD1	x				x	0.27	0.11	0.62	1.00	0.00	0.00	1.03	1.13	0.07	*	*	0.07
8 FCGR2A		x			x	1.00	0.00	0.00	0.00	0.00	1.00	*	*	0.07	1.28	1.13	0.07
9 ATP8B4		x				1.00	0.00	0.00	0.44	0.44	0.13	*	*	0.07	0.74	0.91	0.07
10 C10orf90		x				1.00	0.00	0.00	0.44	0.12	0.44	0.96	0.63	3.63	1.28	1.22	3.59
11 CD82		x				1.00	0.00	0.00	0.00	1.00	0.00	*	*	0.04	0.75	0.91	0.04
12 CNTNAP4		x				1.00	0.00	0.00	0.00	1.00	0.00	*	*	4.26	0.67	0.77	4.21
13 CXCR4		x				1.00	0.00	0.00	0.00	0.00	1.00	1	1.05	0.05	1.55	1.1	0.05
14 DLGAP1		x				1.00	0.00	0.00	0.00	0.00	1.00	*	*	1.53	1.49	1.19	1.53
15 DPP10		x				0.58	0.13	0.29	0.00	0.00	1.00	2.2	1.15	3.08	2.56	1.23	3.06
16 EFCAB6		x				1.00	0.00	0.00	0.00	1.00	0.00	0.94	0.86	1.30	0.76	0.79	1.29
17 FIGN		x				1.00	0.00	0.00	0.00	0.00	1.00	*	*	1.84	1.51	1.18	1.83
18 FRAS1		x				1.00	0.00	0.00	0.00	0.00	1.00	0.99	0.8	2.89	1.59	1.21	2.89
19 JARID2		x				1.00	0.00	0.00	0.00	0.00	1.00	*	*	0.06	1.42	1.1	0.06
20 LRFN5		x				1.00	0.00	0.00	0.00	1.00	0.00	*	*	4.52	0.67	0.77	4.46
21 PTPRN2		x				1.00	0.00	0.00	0.00	0.00	1.00	*	*	0.20	1.67	1.16	0.19
22 RIN3		x				1.00	0.00	0.00	0.00	1.00	0.00	*	*	0.26	0.71	0.86	0.26
23 VRK2		x				1.00	0.00	0.00	0.00	1.00	0.00	*	*	0.09	0.75	0.9	0.09

mitochondrial function (Bose and Beal, 2019; Zaltieri et al., 2015), stress responses (Zhao et al., 2010; Chang et al., 2020), autophagy (Liu et al., 2008; Wang et al., 2016), vesicular trafficking and endocytosis (Perrett et al., 2015; Esposito et al., 2012). Three of these genes (*CDIP1*, *CNTNAP2*, *DUSP1*) have connections with PD in the literature (Li et al., 2022; Brehm et al., 2015; Usenko et al., 2021). The other genes collectively play roles in pathways previously associated with Parkinson’s disease, rendering them plausible candidates for further investigation. The estimated effect sizes (conditional on inclusion in the respective non-null groups) are reported in Table 1 which contains the union of genes identified as non-null by the three-groups joint models.

The joint three-groups with non-local priors identifies 21 interesting genes in the joint MM. Eighteen of these 21 genes were in either the beneficial (8 genes) or deleterious (10 genes) groups for all 10,000 post burn-in MCMC iterations. The other three genes were in each of the three groups for at least 10% of the MCMC iterations. Five of the 21 interesting genes are also identified in the local model (*CDIP1*, *CHCHD6*, *CNTNAP2*, *DUSP1*, and *FAM49B*). *CNTNAP4*, *CXCR4*, *FCGR2A*, and *PTPRN2* are linked to PD in the literature (Hu et al., 2024; Ma et al., 2023; Schilder and Raj, 2022; Kochmanski et al., 2022, and references therein). *EFCAB6* has been studied in connection with a mutation known to be associated with early-onset PD in Strobbe et al. (2018). Several others can be linked to pathways which have been studied in relationship with PD though we are unaware of work which directly links these other genes to PD. These pathway links include *ATP8B4*’s association with the innate immune system, *FRAS1*’s link to ERK signaling, and *JARID2*’s interaction with the Polycomb repressive complex 2, all of which have been implicated or have relation to PD in Liu et al. (2021); Tan et al. (2020); Albert-Gascó et al. (2020); Toskas et al. (2022) respectively.

As expected, there are differences between the genes identified as non-null between the local and non-local versions of our model. Estimated gene effects for gene *IFRD1* and *SYTL3* (Table 1) suggest that some of this discrepancy is due to the difference in behavior between the two priors near zero, as the data in these two cases suggest small but non-null effect sizes; this difference is baked into the design of the non-local priors. There are other genes which do not appear to fit this pattern, and we conjecture that the differences may be attributable to interactions among genes estimated as non-null, which alter the likelihood values. These differences are not surprising when considering that the

standard methods also report gene lists that are not consistent. Additional results and volcano plots are available in the supplementary material.

6 Discussion

Structuring models for data conditional on the three-groups framework has advantages of flexibility, modular incorporation of multiple experimental data types, and the automatic multiplicity adjustment. By combining information across genomic, transcriptomic, and potentially other data types, it provides an increase in power for improved prioritization of genes that show evidence of involvement in disease. Furthermore, using the three-groups model as a platform, in the future we can combine functional data from future cell-based studies and screens that directly assess the impact of a function of a gene on a cell's biological outcome, such as health, morphology, stress response, and proteostasis. In this way, we can harness the power of cell biology together with human genetics and gene expression. Additionally, the Bayesian formulation and use of MCMC allow for inclusion of genes that have observations in some but not all experimental data types.

One challenge that we faced was the computational burden running MCMC on this model; each run on the PD dataset used around 30Gb of RAM and took several days to finish. In the context of a years-long collaboration like ours, this is not a huge problem, but it is inconvenient at the very least. Using NIMBLE's RJMCMC features reduced the computational time significantly, but not enough to make the sampler practical in casual settings. Previous implementations of non-local selection priors saved time by approximately marginalizing out the effect sizes with Laplace approximation schemes (Johnson and Rossell, 2012; Nikooienejad et al., 2016; Shin et al., 2018). This was unappealing in our context because the effect sizes are important in our experimental context.

One issue that requires further attention is the effectiveness of our scheme for mapping between SNVs and genes in either GWAS or whole genome sequencing (WGS) datasets, particularly for SNVs in non-coding regions. The technique that we used (Section 2.3) for mapping SNVs into genes is simplistic and could result in missed signals if SNVs within a single gene work in opposite directions. Other mapping techniques may enrich the procedure.

The strategy of combining genomic, transcriptomic, phenotypic, and potentially other sources of information using the three-groups framework can be applied to any heritable disease with multiple data types available. The PD datasets that we analyzed here are publicly available, but others like family pedigree WGS have been collected by our lab, and still others, including small interfering RNA screen, will result from follow-up experiments.

Acknowledgements

This work was made possible by the NSF collaborative grant NSF-1761941/2309825. Additional support for this work came from NIH R01 LM013617, R01 NS124848, the Michael J Fox Foundation, and CIRM DISC0-16039. Data used in the preparation of this article were obtained 09/21/2018 from the Parkinson's Progression Markers Initiative (PPMI) database (www.ppmi-info.org/access-data-specimens/download-data), RRID:SCR 006431. For up-to-date information on the study, visit www.ppmi-info.org.

Supporting Information

Web Appendices, Tables, and Figures referenced in Sections 4, 5, and some additional information is available with this paper on the arXiv.

References

- Agarwal, D., Sandor, C., Volpato, V., Caffrey, T. M., Monzón-Sandoval, J., Bowden, R., Alegre-Abarrategui, J., Wade-Martins, R., and Webber, C. (2020). A single-cell atlas of the human substantia nigra reveals cell-specific pathways associated with neurological disorders. *Nature communications*, 11(1):4183–4183.
- Albert-Gascó, H., Ros-Bernal, F., Castillo-Gómez, E., and Olucha-Bordonau, F. E. (2020). MAP/ERK signaling in developing cognitive and emotional function and its effect on pathological and neurodegenerative processes. *International journal of molecular sciences*, 21(12):4471.
- Asimit, J. L., Day-Williams, A. G., Morris, A. P., and Zeggini, E. (2012). ARIEL and AMELIA: testing for an accumulation of rare variants using next-generation sequencing data. *Human Heredity*, 73(2):84–94.
- Barbieri, M. M. and Berger, J. O. (2004). Optimal predictive model selection. *The Annals of statistics*, 32(3):870–897.
- Benjamini, Y. and Heller, R. (2008). Screening for partial conjunction hypotheses. *Biometrics*, 64(4):1215–1222.

- Benjamini, Y. and Hochberg, Y. (1995). Controlling the false discovery rate: a practical and powerful approach to multiple testing. *Journal of the Royal Statistical Society Series B-Statistical Methodology*, 57(1):289–300.
- Bose, A. and Beal, M. F. (2019). Mitochondrial dysfunction and oxidative stress in induced pluripotent stem cell models of Parkinson’s disease. *European Journal of Neuroscience*, 49(4):525–532.
- Boyle, E. A., Li, Y. I., and Pritchard, J. K. (2017). An expanded view of complex traits: From polygenic to omnigenic. *Cell*, 169(7):1177–1186.
- Brehm, N., Bez, F., Carlsson, T., Kern, B., Gispert, S., Auburger, G., and Cenci, M. (2015). A genetic mouse model of Parkinson’s disease shows involuntary movements and increased postsynaptic sensitivity to apomorphine. *Molecular neurobiology*, 52:1152–1164.
- Chang, M., Zhang, Y., Hui, Z., Wang, D., and Guo, H. (2020). IFRD1 regulates the asthmatic responses of airway via NF- κ B pathway. *Molecular Immunology*, 127:186–192.
- Clayton, D. F. and George, J. M. (1998). The synucleins: a family of proteins involved in synaptic function, plasticity, neurodegeneration and disease. *Trends in neurosciences*, 21(6):249–254.
- de Valpine, P., Paciorek, C., Turek, D., Michaud, N., Anderson-Bergman, C., Obermeyer, F., Wehrhahn Cortes, C., Rodríguez, A., Temple Lang, D., and Paganin, S. (2023). *NIMBLE: MCMC, Particle Filtering, and Programmable Hierarchical Modeling*. R package version 1.0.1.
- de Valpine, P., Turek, D., Paciorek, C., Anderson-Bergman, C., Lang, D. T., and Bodik, R. (2017). Programming with models: writing statistical algorithms for general model structures with NIMBLE. *Journal of Computational and Graphical Statistics*, 26:403–413.
- Ding, D. Y., Li, S., Narasimhan, B., and Tibshirani, R. (2022). Cooperative learning for multiview analysis. *Proceedings of the National Academy of Sciences*, 119(38):e2202113119.
- Efron, B., Tibshirani, R., Storey, J. D., and Tusher, V. (2001). Empirical bayes analysis of a microarray experiment. *Journal of the American Statistical Association*, 96(456):1151–1160.
- Esposito, G., Ana Clara, F., and Verstreken, P. (2012). Synaptic vesicle trafficking and Parkinson’s disease. *Developmental neurobiology*, 72(1):134–144.
- Fisher, R. (1929). Tests of significance in harmonic analysis. *Proceedings of the Royal Society of London Series A-Mathematical and Physical Sciences*, 125(796):54–59.
- Gazal, S., Weissbrod, O., Hormozdiari, F., Dey, K. K., Nasser, J., Jagadeesh, K. A., Weiner, D. J., Shi, H., Fulco, C. P., O’Connor, L. J., et al. (2022). Combining snp-to-gene linking strategies to identify disease genes and assess disease omnigenicity. *Nature genetics*, 54(6):827–836.
- Gelman, A. (2014). *Bayesian data analysis*. YBP Print DDA. CRC Press, Boca Raton, third edition.
- Genovese, C. and Wasserman, L. (2004). A stochastic process approach to false discovery control. *The Annals of Statistics*, 32(3):1035–1061.
- Gerard, D. (2020). Data-based RNA-seq simulations by binomial thinning. *BMC bioinformatics*, 21(1):206–206.
- Gneiting, T. and Raftery, A. E. (2007). Strictly proper scoring rules, prediction, and estimation. *Journal of the American Statistical Association*, 102(477):359–378.
- Green, P. J. (1995). Reversible jump Markov chain Monte Carlo computation and Bayesian model determination. *Biometrika*, 82(4):711–732.
- Holzinger, E. R., Dudek, S. M., Frase, A. T., Pendergrass, S. A., and Ritchie, M. D. (2013). Athena: the analysis tool for heritable and environmental network associations. *Bioinformatics*, 30(5):698–705.
- Hu, W., Wang, M., Sun, G., Zhang, L., and Lu, H. (2024). Early b cell factor 3 (EBF3) attenuates Parkinson’s disease through directly regulating contactin-associated protein-like 4 (CNTNAP4) transcription: An experimental study. *Cellular Signalling*, pages 111–139.
- Johnson, V. E. and Rossell, D. (2012). Bayesian model selection in high-dimensional settings. *Journal of the American Statistical Association*, 107(498):649–660.
- Johnson, V. E. E. and Rossell, D. (2010). On the use of non-local prior densities in bayesian hypothesis tests. *Journal of the Royal Statistical Society. Series B, Statistical methodology*, 72(2):143–170.
- Kochmanski, J., Kuhn, N. C., and Bernstein, A. I. (2022). Parkinson’s disease-associated, sex-specific changes in DNA methylation at PARK7 (DJ-1), SLC17A6 (VGLUT2), PTPRN2 (IA-2 β), and NR4A2 (NURR1) in cortical neurons. *npj Parkinson’s Disease*, 8(1):120.

- Law, C. W., Chen, Y., Shi, W., and Smyth, G. K. (2014). voom: precision weights unlock linear model analysis tools for rna-seq read counts. *Genome biology*, 15(2):R29–R29.
- Li, B. and Leal, S. M. (2008). Methods for detecting associations with rare variants for common diseases: application to analysis of sequence data. *The American Journal of Human Genetics*, 83(3):311–321.
- Li, L., Wang, H., Li, H., Lu, X., Gao, Y., and Guo, X. (2022). Long noncoding rna bace1-antisense transcript plays a critical role in Parkinson’s disease via microRNA-214-3p/cell death-inducing p53-target protein 1 axis. *Bioengineered*, 13(4):10889–10901.
- Li, W. and Chekouo, T. (2022). Bayesian group selection with non-local priors. *Computational statistics*, 37(1):287–302.
- Li, Y., Wu, F.-X., and Ngom, A. (2018). A review on machine learning principles for multi-view biological data integration. *Briefings in bioinformatics*, 19(2):325–340.
- Liu, H., Ho, P. W.-L., Leung, C.-T., Pang, S. Y.-Y., Chang, E. E. S., Choi, Z. Y.-K., Kung, M. H.-W., Ramsden, D. B., and Ho, S.-L. (2021). Aberrant mitochondrial morphology and function associated with impaired mitophagy and DNMI1L-MAPK/ERK signaling are found in aged mutant Parkinsonian LRRK2R1441G mice. *Autophagy*, 17(10):3196–3220.
- Liu, Y.-X., Wang, J., Guo, J., Wu, J., Lieberman, H. B., and Yin, Y. (2008). DUSP1 is controlled by p53 during the cellular response to oxidative stress. *Molecular Cancer Research*, 6(4):624–633.
- Love, M. I., Huber, W., and Anders, S. (2014). Moderated estimation of fold change and dispersion for rna-seq data with deseq2. *Genome biology*, 15(12):550–550.
- Ma, J., Dong, L., Chang, Q., Chen, S., Zheng, J., Li, D., Wu, S., Yang, H., and Li, X. (2023). CXCR4 knockout induces neuropathological changes in the MPTP-lesioned model of Parkinson’s disease. *Biochimica et Biophysica Acta (BBA)-Molecular Basis of Disease*, 1869(2):166597.
- Madsen, B. E. and Browning, S. R. (2009). A groupwise association test for rare mutations using a weighted sum statistic. *PLoS Genetics*, 5(2):e1000384.
- Mochizuki, H., Goto, K., Mori, H., and Mizuno, Y. (1996). Histochemical detection of apoptosis in Parkinson’s disease. *Journal of the neurological sciences*, 137(2):120–123.
- Montgomery, S. B., Dermitzakis, E. T., Sammeth, M., Gutierrez-Arcelus, M., Lach, R. P., Ingle, C., Nisbett, J., and Guigo, R. (2010). Transcriptome genetics using second generation sequencing in a caucasian population. *Nature (London)*, 464(7289):773–777.
- Morais, V. A., Verstreken, P., Roethig, A., Smet, J., Snellinx, A., Vanbrabant, M., Haddad, D., Frezza, C., Mandemakers, W., Vogt-Weisenhorn, D., et al. (2009). Parkinson’s disease mutations in PINK1 result in decreased complex I activity and deficient synaptic function. *EMBO molecular medicine*, 1(2):99–111.
- Morgenthaler, S. and Thilly, W. G. (2007). A strategy to discover genes that carry multi-allelic or mono-allelic risk for common diseases: a cohort allelic sums test (cast). *Mutation Research/Fundamental and Molecular Mechanisms of Mutagenesis*, 615(1):28–56.
- Nalls, M. A., Pankratz, N., Lill, C. M., Do, C. B., Hernandez, D. G., Saad, M., DeStefano, A. L., Kara, E., Bras, J., Sharma, M., Schulte, C., Keller, M. F., Arepalli, S., Letson, C., Edsall, C., Stefansson, H., Liu, X., Pliner, H., Lee, J. H., Cheng, R., Ikram, M. A., Ioannidis, J. P. A., Hadjigeorgiou, G. M., Bis, J. C., Martinez, M., Perlmutter, J. S., Goate, A., Marder, K., Fiske, B., Sutherland, M., Xiromerisiou, G., Myers, R. H., Clark, L. N., Stefansson, K., Hardy, J. A., Heutink, P., Chen, H., Wood, N. W., Houlden, H., Payami, H., Brice, A., Scott, W. K., Gasser, T., Bertram, L., Eriksson, N., Foroud, T., and Singleton, A. B. (2014). Large-scale meta-analysis of genome-wide association data identifies six new risk loci for Parkinson’s disease. *Nature genetics*, 46(9):989–+.
- Nikooienejad, A., Wang, W., and Johnson, V. E. (2016). Bayesian variable selection for binary outcomes in high-dimensional genomic studies using non-local priors. *BIOINFORMATICS*, 32(9):1338–1345.
- Perrett, R. M., Alexopoulou, Z., and Tofaris, G. K. (2015). The endosomal pathway in Parkinson’s disease. *Molecular and Cellular Neuroscience*, 66:21–28.
- Pickrell, J. K., Gilad, Y., Pritchard, J. K., Marioni, J. C., Pai, A. A., Degner, J. F., Engelhardt, B. E., Nkadori, E., Veyrieras, J.-B., and Stephens, M. (2010). Understanding mechanisms underlying human gene expression variation with rna sequencing. *Nature (London)*, 464(7289):768–772.
- Richardson, S., Tseng, G. C., and Sun, W. (2016). Statistical methods in integrative genomics. *Annual review of statistics and its application*, 3:181–209.
- Ritchie, M. D., Holzinger, E. R., Li, R., Pendergrass, S. A., and Kim, D. (2015). Methods of integrating data to uncover genotype-phenotype interactions. *Nature Reviews. Genetics*, 16(2):85.

- Robinson, M. D., McCarthy, D. J., and Smyth, G. K. (2010). edgeR: a bioconductor package for differential expression analysis of digital gene expression data. *BIOINFORMATICS*, 26(1):139–140.
- Schilder, B. M. and Raj, T. (2022). Fine-mapping of Parkinson’s disease susceptibility loci identifies putative causal variants. *Human Molecular Genetics*, 31(6):888–900.
- Scott, J. G. and Berger, J. O. (2010). Bayes and empirical-Bayes multiplicity adjustment in the variable-selection problem. *The Annals of Statistics.*, 38(5):2587–2619.
- Shin, M., Bhattacharya, A., and Johnson, V. E. (2018). Scalable Bayesian variable selection using nonlocal prior densities in ultrahigh-dimensional settings. *Statist. Sinica*, 28(2):1053–1078.
- Stouffer, S. A., Suchman, E. A., DeVinney, L. C., Star, S. A., and Williams Jr, R. M. (1949). The American soldier: Adjustment during army life, Vol. I. *Studies in Social Psychology World War II*.
- Strobbe, D., Robinson, A. A., Harvey, K., Rossi, L., Ferraina, C., De Biase, V., Rodolfo, C., Harvey, R. J., and Campanella, M. (2018). Distinct mechanisms of pathogenic DJ-1 mutations in mitochondrial quality control. *Frontiers in Molecular Neuroscience*, 11:68.
- Tan, E.-K., Chao, Y.-X., West, A., Chan, L.-L., Poewe, W., and Jankovic, J. (2020). Parkinson disease and the immune system—associations, mechanisms and therapeutics. *Nature Reviews Neurology*, 16(6):303–318.
- Tatton, W. G., Chalmers-Redman, R., Brown, D., and Tatton, N. (2003). Apoptosis in Parkinson’s disease: signals for neuronal degradation. *Annals of Neurology: Official Journal of the American Neurological Association and the Child Neurology Society*, 53(S3):S61–S72.
- Toskas, K., Yaghmaeian-Salmani, B., Skiteva, O., Paslawski, W., Gillberg, L., Skara, V., Antoniou, I., Södersten, E., Svenningsson, P., Chergui, K., et al. (2022). PRC2-mediated repression is essential to maintain identity and function of differentiated dopaminergic and serotonergic neurons. *Science Advances*, 8(34):eabo1543.
- Tyekucheva, S., Marchionni, L., Karchin, R., and Parmigiani, G. (2011). Integrating diverse genomic data using gene sets. *Genome biology*, 12(10):R105–R105.
- Uffelmann, E., Huang, Q. Q., Munung, N. S., De Vries, J., Okada, Y., Martin, A. R., Martin, H. C., Lappalainen, T., and Posthuma, D. (2021). Genome-wide association studies. *Nature Reviews Methods Primers*, 1(1):59.
- Usenko, T., Bezrukova, A., Basharova, K., Panteleeva, A., Nikolaev, M., Kopytova, A., Miliukhina, I., Emelyanov, A., Zakharova, E., and Pchelina, S. (2021). Comparative transcriptome analysis in monocyte-derived macrophages of asymptomatic gba mutation carriers and patients with GBA-associated Parkinson’s disease. *Genes*, 12(10):1545.
- Wang, J., Zhou, J.-Y., Kho, D., Reiners Jr, J. J., and Wu, G. S. (2016). Role for DUSP1 (dual-specificity protein phosphatase 1) in the regulation of autophagy. *Autophagy*, 12(10):1791–1803.
- Zaltieri, M., Longhena, F., Pizzi, M., Missale, C., Spano, P., Bellucci, A., et al. (2015). Mitochondrial dysfunction α -Synuclein synaptic pathology in Parkinson’s disease: who’s on first? *Parkinson’s disease*, 2015.
- Zhao, C., Datta, S., Mandal, P., Xu, S., and Hamilton, T. (2010). Stress-sensitive regulation of IFRD1 mRNA decay is mediated by an upstream open reading frame. *Journal of Biological Chemistry*, 285(12):8552–8562.

Appendix: Data Generation for Simulations

We simulated GWAS datasets from a standard logistic regression model. This scenario is idealistic in that we fit the exact data-generating response model; however the standard GWAS pipeline also fits this data-generating response model, so comparisons between our three-groups approach and standard GWAS are on an even footing. To generate the binary predictor variables, which indicate the presence (or absence) of any minor alleles, we simulated a gene-wise minor allele frequency from a Beta(20, 35) distribution, which has most of its mass between 0.2 and 0.5 (i.e., for $X \sim \text{Beta}(20, 35)$, $P\{X \in (0.2, 0.5)\} = 0.977$). Then, conditional on the minor allele frequency, we simulated the binary predictor for each individual for that gene from a Bernoulli distribution with success probability equal to the minor allele frequency. Next, the probability of being in the treatment group is simulated from a Bernoulli distribution with success probability equal to the inverse logit of a linear combination of a normally distributed intercept and the predictors, multiplied by the fixed gene effects. The sign of the gene effects indicates group membership, with positive effects being deleterious and negative effects being beneficial.

To make things as realistic as possible, we generated the RNA-seq data from subsets of a real RNA-seq dataset. This involved selecting 250 genes from an RNA-seq dataset and adding signal to the genes which should be included in the beneficial and deleterious groups. We started with the combined data from Pickrell et al. (2010) and Montgomery et al. (2010) (<https://bowtie-bio.sourceforge.net/recount/>), as this dataset has a large number of biological replicates (129) and many genes (11,107). We added signal using a binomial thinning scheme, as in Gerard (2020),

Table 2: Additional three-groups models

Label	Effect size distributions	Hyper-parameters	Is local?	Is symmetric?
nonL piMOM	half-piMOM	$\tau \sim$ half-piMOM	non-local	asymmetric
nonL invG	half-piMOM	$\tau \sim$ inverse Gamma	non-local	asymmetric
nonL fixed	half-piMOM	fixed	non-local	symmetric
local piMOM	half-Normal	$\mu \sim$ inverse Gamma $\sigma \sim$ half-piMOM	local	asymmetric
local fixed	half-Normal	fixed	local	symmetric

using the referenced R package `seqgendiff`. This method allows the simulated data to retain the characteristics of real RNA-seq data and does not bias results towards one method or another.

Appendix: Additional Simulations

We ran several additional versions of the three-groups model and report results here. The main text includes an asymmetric non-local three-groups model which has half-piMOM effect size distributions ($f^{(m)-}$ and $f^{(m)+}$) with separate half-piMOM hyper-priors placed on the scaling parameter τ . This model is compared to a symmetric local three-groups model which has half-normal effect size distributions that are fixed. In this appendix we compare these models to another asymmetric non-local model that instead has inverse gamma hyper-priors on the τ parameters, a symmetric non-local model that has fixed τ values, and an asymmetric local model that has separate inverse gamma hyper-priors on the means and separate half-piMOM hyper-priors on the standard deviations of the half-normal effect size priors. Table 2 demonstrates the distinctions between these models. We do not include results from an asymmetric local model which had separate inverse gamma hyper-priors on the means and standard deviations as they were uniformly worse and made the plots unreadable.

These simulations are compared using the same metrics that were discussed in section 4 of the main text; the logarithmic score, brier score, area under the receiver operating characteristic curve, and the true positive rate at two different fixed mean false positive rates (Figure 5). These plots demonstrate a range of choices (for modelling the effect sizes) which provide comparable results. This range illustrates that most of the benefit of our method comes from the borrowing of strength across data types using three-groups structure.

While there are many similarities between these plots we think that it is worth highlighting a few differences. The non-local model with inverse gamma hyper-priors required tuning of the hyper-parameter values; we had to move the mass away from zero to ensure the posterior distributions for τ were not nearly zero. This suggests to us that the sparsity invoked by the automatic multiplicity correction of the Dirichlet-categorical inclusion scheme can become swamped by many very small empirical effect sizes. In other words, some engineering is required to ensure that the effect size distributions do not become additional "spikes" at trivially small values.

Appendix: RJMCMC comments

Our numerical implementation used NIMBLE's RJMCMC which required some additional customization. Gene's in the null group have effect sizes of zero. Our numerical implementation requires beneficial and deleterious effect sizes at every MCMC iteration. These effect sizes are zeroed out for gene's which are in the null group in an intermediary step in each iteration. We used NIMBLE's RJMCMC in order to cut out this unnecessary computation. Unfortunately the RJMCMC does not actually shrink the parameter space but instead fixes the excluded parameters at some pre-specified value (zero by default). In our case this fixes the beneficial and deleterious effect sizes at zero. Updating the hyper-parameter values (e.g., τ) requires a likelihood calculation which includes all of these fixed values. This results in errors for the default settings due to the non-local effect-size distributions. We wrote custom distributions which set the log-likelihood at zero for all effects which are set by the RJMCMC toggler to fix this issue. This results in equivalent likelihood calculations to those from the true shrunk parameter space.

Appendix: Volcano Plots

It is common to use volcano plots to identify the most promising genes in RNA-seq analyses. These plots conventionally have the log fold change on the horizontal axis and the negative log p-value on the vertical axis which allows investigators

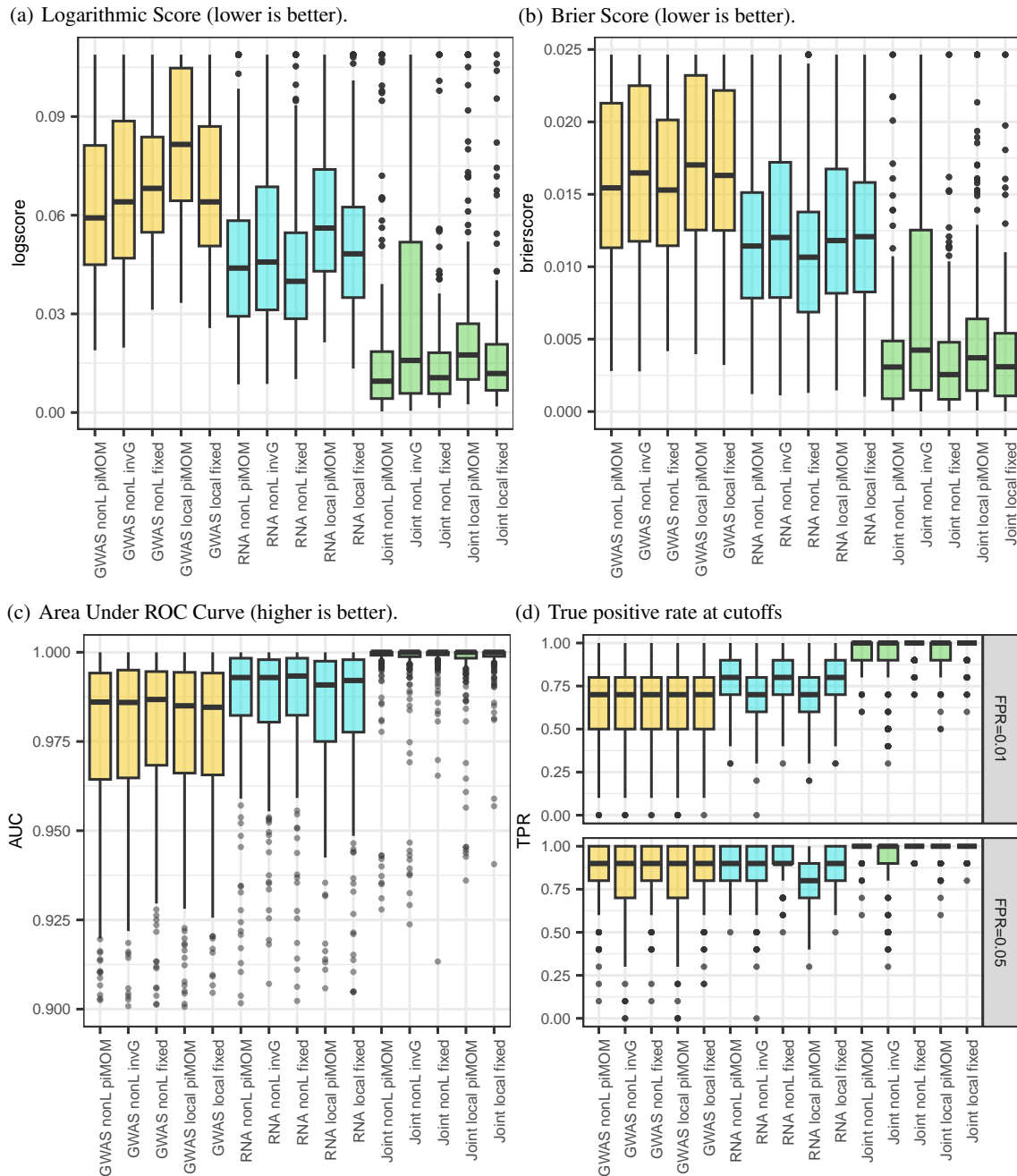


Figure 5: Boxplots of logarithmic scores (a), Brier scores (b), area under receiver operating characteristic curve (c) computed from posterior probability of inclusion in the null group, and the true positive rates (i.e. power) computed at classification cutoffs that result in mean false positive rates of 0.01 (top panel) and 0.05 (bottom panel) in (d) as in Figure 4 in the main text.

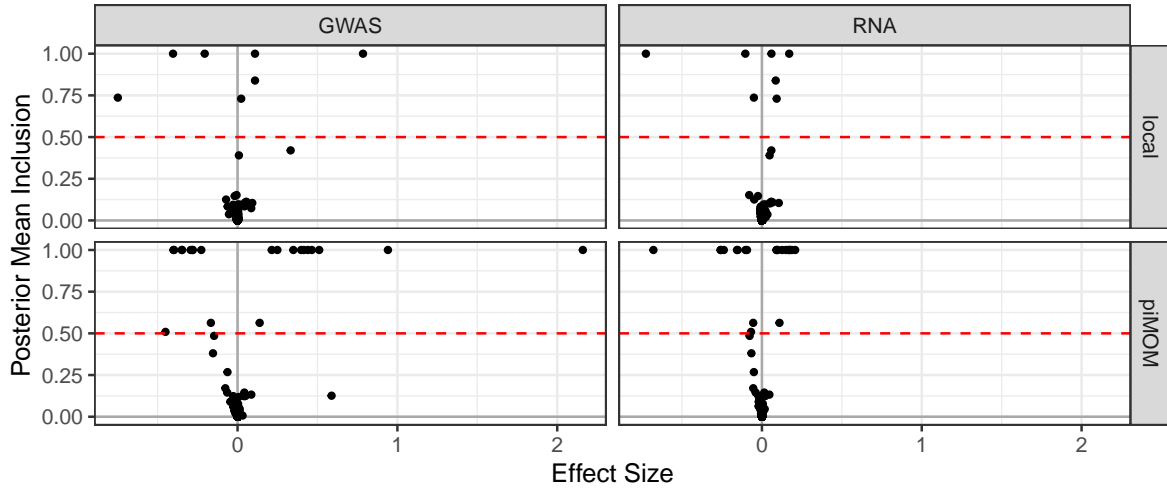


Figure 6: Volcano plots for the local model (top row) and piMOM model (bottom row). Effect sizes are the marginal log odds ratio (GWAS) and log fold change (RNA). The red dashed line indicates the MM cutoff.

to quickly subset genes which are both statistically significant and have large effect sizes. Our method does not benefit from these plots in the same manner due to the inherent sparsity. Nevertheless, we have created a version of these plots in Figure 6 with the marginal log effect size on the horizontal axis and posterior mean of inclusion on the vertical axis. The vast majority of genes are not visible because they are piled up exactly at the origin. These plots highlight the non-local nature of the piMOM model; no included genes have small effect sizes.

Appendix: Non-null genes from all models

Gene	TG RNA local	TG RNA piMOM	TG GWAS local	TG GWAS piMOM	TG joint local	TG joint piMOM	edgeR	voom	DESeq2	GWAS	GWAS+edgeR	GWAS+voom	GWAS+DESeq2
1 ACTR10			*										
2 ADAMTS19			*										
3 AFF3									*				
4 ALOX5AP			*						*				
5 ANK3			*										
6 ANKFN1				*									
7 AOAH			*										
8 APOD	*						*				*		
9 ARF1			*										
10 ARHGEF26			*										
11 ATP2B1			*										
12 ATP2C1			*										
13 ATP5A1			*										
14 ATP6V0B								*	*				
15 ATP8B4						*							
16 AZI2				*									
17 BDH1			*										
18 C10orf90						*							
19 C2CD5			*										
20 C6orf136			*										
21 CAMLG			*										
22 CAMTA1				*									

Continued on next page

Gene	TG RNA local	TG RNA piMOM	TG GWAS local	TG GWAS piMOM	TG joint local	TG joint piMOM	edgeR	voom	DESeq2	GWAS	GWAS+edgeR	GWAS+voom	GWAS+DESeq2
23	CANX			*									
24	CCDC136			*									
25	CCPG1			*					*				
26	CD180								*				
27	CD200	*	*				*						
28	CD82					*							
29	CD83	*					*				*		
30	CDH7			*						*			
31	CDIP1				*	*				*	*	*	*
32	CDK14				*	*			*				
33	CHCHD3			*									
34	CHCHD6			*	*	*				*	*	*	*
35	CHD6			*	*	*							
36	CLEC7A								*		*	*	*
37	CNTNAP2	*	*		*	*	*			*	*	*	*
38	CNTNAP4				*	*							
39	CNTNAP5			*	*	*			*				
40	CREM				*	*			*				
41	CSMD1				*	*							
42	CTSB			*									
43	CXCR4					*							
44	CYB5R1			*									
45	DACH1				*	*							
46	DDIT3			*									
47	DLGAP1					*							
48	DOCK4					*	*	*					
49	DPP10					*							
50	DPYSL5			*		*				*	*	*	*
51	DUSP1	*		*	*	*	*	*		*	*	*	*
52	EDIL3				*	*							
53	EFCAB6					*							
54	EFEMP1			*									
55	ENPP2			*									
56	EVL			*									
57	FAM49B				*	*			*				
58	FAM98A			*									
59	FBXL17			*									
60	FCGR2A					*			*				*
61	FGD4	*				*	*	*		*	*	*	*
62	FIGN					*							
63	FILIP1L					*	*						
64	FMNL3			*									
65	FNDC3A			*									*
66	FOCAD				*	*							
67	FOS					*	*	*		*	*	*	*
68	FRAS1			*		*							
69	FSD1			*									
70	FSTL5				*	*							
71	GABARAPL1	*				*	*	*			*	*	*
72	GABRG3			*									
73	GALNT13			*	*	*							
74	GLIS3				*	*							
75	GNB4							*					
76	GPR183			*									
77	GRIA2			*									
78	HAGH			*									
79	HAP1			*									

Continued on next page

	Gene	TG RNA local	TG RNA piMOM	TG GWAS local	TG GWAS piMOM	TG joint local	TG joint piMOM	edgeR	voom	DESeq2	GWAS	GWAS+edgeR	GWAS+voom	GWAS+DESeq2
80	HDAC9				*									
81	HERPUD1									*				
82	HIF1A									*				
83	HLA-DPA1			*						*				
84	HSPA2			*										
85	HSPA6				*						*	*	*	*
86	HSPD1													*
87	IDH3A			*						*				*
88	IFIT3							*		*				*
89	IFRD1	*				*		*	*	*				*
90	IQCA1			*						*				
91	ITM2B									*				
92	JARID2						*							
93	JPH4			*										
94	KATNB1			*										
95	KBTBD8			*										
96	KCNJ6			*										
97	KHDC1			*										
98	KHDRBS3			*										
99	KIAA1958										*		*	*
100	KLF6									*				*
101	KLK6			*						*				*
102	LAPTM5			*						*				*
103	LIN7A									*			*	*
104	LINC01197			*						*				*
105	LPAR6			*						*				*
106	LPCAT2									*				*
107	LRFN5						*			*				*
108	LRRK2									*				*
109	LRRN1			*						*				*
110	LYRM1									*			*	*
111	MAP2K4									*				*
112	MAP4K5			*						*				*
113	MARCKSL1			*						*				*
114	MAST2				*					*				*
115	MCTP1							*		*			*	*
116	MFSD4A			*						*				*
117	MOCS2			*						*				*
118	MRPL55			*						*				*
119	MXD1									*				*
120	NCALD			*						*				*
121	NKAIN2			*						*				*
122	NPTN									*			*	*
123	NSF			*						*				*
124	NUTF2			*						*				*
125	OR2W3									*				*
126	ORMDL1			*						*				*
127	PACSIN1			*						*				*
128	PARP8									*				*
129	PCSK5				*					*				*
130	PDK2									*				*
131	PDK4									*			*	*
132	PELI1	*						*	*	*			*	*
133	PGAM1		*							*				*
134	PLEKHB1		*							*				*
135	PLEKHB2		*							*				*
136	PLXDC2									*				*

Continued on next page

	Gene	TG RNA local	TG RNA piMOM	TG GWAS local	TG GWAS piMOM	TG joint local	TG joint piMOM	edgeR	voom	DESeq2	GWAS	GWAS+edgeR	GWAS+voom	GWAS+DESeq2
137	PTPRD				*									
138	PTPRG				*									
139	PTPRN2						*							
140	PTPRR				*									
141	RAMP1			*	*									
142	RANBP2			*	*									
143	RAP1GAP	*	*					*		*		*		*
144	RGS2				*					*				
145	RHOQ			*										
146	RIN3						*							
147	RNF13									*				
148	RSRP1				*					*				*
149	S100B			*	*									
150	SCN1A			*	*									
151	SCRN2			*	*									
152	SEMA3B			*	*									
153	SERINC3			*	*									
154	SKAP2			*	*					*				
155	SLC16A4							*						
156	SLC24A2				*									
157	SLC25A29			*										
158	SLC31A2									*				
159	STRBP							*		*				
160	SYT13			*	*									
161	SYT5			*	*									
162	SYTL3					*		*		*		*		*
163	TIMM22			*	*									
164	TLR6			*	*					*				*
165	TM2D3									*				*
166	TMCC3									*				*
167	TMEM125			*	*									
168	TMEM181			*	*									
169	TMEM246			*	*									
170	TMTC1				*									
171	TMX4									*				
172	TPI1			*	*									
173	TPST1							*		*		*		*
174	TRANK1									*				
175	TRPS1			*	*									
176	TUFM			*	*									
177	TYROBP									*				
178	UQCR10			*	*									
179	UQCRC1			*	*									
180	VRK2						*							
181	WDR12			*	*					*				
182	XYLTI				*									
183	ZDHHC20			*	*									

Table 3: Genes identified as non-null in at least one of model. A gene is classified as non-null in all models with an “*”. The three groups (TG) models use the median model (cutoff at $P_{null} < 0.5$) except for the local GWAS model which included too many genes. We used a cutoff of 0.0001 for this GWAS model which still included 94 genes. All conventional models used a cutoff of 0.05.

Appendix: Non-null genes and effect sizes from TG RNA only and GWAS only models.

Gene	P^{null} RNA local	P^{ben} RNA local	P^{del} RNA local	P^{null} RNA piMOM	P^{ben} RNA piMOM	P^{del} RNA piMOM	P^{null} GWAS local	P^{ben} GWAS local	P^{del} GWAS local	P^{null} GWAS piMOM	P^{ben} GWAS piMOM	P^{del} GWAS piMOM	RNA effect local	Dispersion local	RNA effect piMOM	Dispersion piMOM	GWAS effect local	GWAS effect piMOM
1 ACTR10	1.00	0.00	0.00	1.00	0.00	0.00	0.00	0.00	1.00	1.00	0.00	0.00	x	x	x	x	179.34	x
2 ADAMTS19	1.00	0.00	0.00	1.00	0.00	0.00	0.00	0.00	1.00	1.00	0.00	0.00	x	x	x	x	2.37	x
3 ALOX5AP	1.00	0.00	0.00	1.00	0.00	0.00	0.00	0.00	1.00	1.00	0.00	0.00	x	x	x	x	0.03	x
4 ANK3	1.00	0.00	0.00	1.00	0.00	0.00	0.00	0.00	1.00	1.00	0.00	0.00	x	x	x	x	3.36	x
5 ANKFN1	1.00	0.00	0.00	1.00	0.00	0.00	0.00	0.00	1.00	1.00	0.00	0.00	x	x	x	x	x	0.71
6 AOA3	1.00	0.00	0.00	1.00	0.00	0.00	0.00	0.00	1.00	1.00	0.00	0.00	x	x	x	x	2.92	x
7 APOD	0.22	0.10	0.68	1.00	0.00	0.00	1.00	0.00	0.00	1.00	0.00	0.00	0.45	5.16	x	x	x	x
8 ARF1	1.00	0.00	0.00	1.00	0.00	0.00	0.00	0.00	1.00	1.00	0.00	0.00	x	x	x	x	20.39	x
9 ARHGAP26	1.00	0.00	0.00	1.00	0.00	0.00	0.00	0.00	1.00	1.00	0.00	0.00	x	x	x	x	1.95	x
10 ATP2B1	1.00	0.00	0.00	1.00	0.00	0.00	0.00	0.00	1.00	1.00	0.00	0.00	x	x	x	x	2.04	x
11 ATP2C1	1.00	0.00	0.00	1.00	0.00	0.00	0.00	0.00	1.00	1.00	0.00	0.00	x	x	x	x	2.43	x
12 ATP5A1	1.00	0.00	0.00	1.00	0.00	0.00	0.00	0.00	1.00	1.00	0.00	0.00	x	x	x	x	0.16	x
13 AZI2	1.00	0.00	0.00	1.00	0.00	0.00	0.00	0.00	1.00	1.00	0.00	0.00	x	x	x	x	x	1.82
14 BDH1	1.00	0.00	0.00	1.00	0.00	0.00	0.00	0.00	1.00	1.00	0.00	0.00	x	x	x	x	0.46	x
15 C2CD5	1.00	0.00	0.00	1.00	0.00	0.00	0.00	0.00	1.00	1.00	0.00	0.00	x	x	x	x	0.08	x
16 C6orf136	1.00	0.00	0.00	1.00	0.00	0.00	0.00	0.00	1.00	1.00	0.00	0.00	x	x	x	x	3.03	x
17 CAMLG	1.00	0.00	0.00	1.00	0.00	0.00	0.00	0.00	1.00	1.00	0.00	0.00	x	x	x	x	0.28	x
18 CAMTA1	1.00	0.00	0.00	1.00	0.00	0.00	0.00	0.00	1.00	1.00	0.00	0.00	x	x	x	x	x	0.41
19 CANX	1.00	0.00	0.00	1.00	0.00	0.00	0.00	0.00	1.00	1.00	0.00	0.00	x	x	x	x	0.03	x
20 CCDC136	1.00	0.00	0.00	1.00	0.00	0.00	0.00	0.00	1.00	1.00	0.00	0.00	x	x	x	x	0.25	x
21 CCPG1	1.00	0.00	0.00	1.00	0.00	0.00	0.00	0.00	1.00	1.00	0.00	0.00	x	x	x	x	2.27	x
22 CD200	0.42	0.46	0.12	0.44	0.49	0.07	1.00	0.00	0.00	1.00	0.00	0.00	0.77	0.43	0.75	0.43	x	x
23 CD83	0.37	0.51	0.12	1.00	0.00	0.00	1.00	0.00	0.00	1.00	0.00	0.00	0.84	0.16	x	x	x	x
24 CDH7	1.00	0.00	0.00	1.00	0.00	0.00	0.00	0.00	1.00	1.00	0.00	0.00	x	x	x	x	5.89	x
25 CDIP1	1.00	0.00	0.00	1.00	0.00	0.00	0.00	0.00	1.00	1.00	0.00	0.00	x	x	x	x	x	0.49
26 CHCHD3	1.00	0.00	0.00	1.00	0.00	0.00	0.00	0.00	1.00	1.00	0.00	0.00	x	x	x	x	2.26	x
27 CHCHD6	1.00	0.00	0.00	1.00	0.00	0.00	0.00	0.00	1.00	1.00	0.00	0.00	x	x	x	x	0.41	0.8

Continued on next page

Gene	P^{null} RNA local	P^{ben} RNA local	P^{del} RNA local	P^{null} RNA piMOM	P^{ben} RNA piMOM	P^{del} RNA piMOM	P^{null} GWAS local	P^{ben} GWAS local	P^{del} GWAS local	P^{null} GWAS piMOM	P^{ben} GWAS piMOM	P^{del} GWAS piMOM	RNA effect local	Dispersion local	RNA effect piMOM	Dispersion piMOM	GWAS effect local	GWAS effect piMOM
28 CHD6	1.00	0.00	0.00	1.00	0.00	0.00	1.00	0.00	1.00	1.00	0.00	0.00	x	x	x	x	2.71	x
29 CNTNAP2	0.22	0.10	0.68	0.00	1.00	0.00	1.00	0.00	0.00	1.00	0.00	0.00	0.48	1.17	0.5	1.16	x	x
30 CNTNAP5	1.00	0.00	0.00	1.00	0.00	0.00	0.00	1.00	0.00	0.39	0.14	0.47	x	x	x	x	5.58	0.61
31 CSMD1	1.00	0.00	0.00	1.00	0.00	0.00	1.00	0.00	0.00	1.00	0.00	0.00	x	x	x	x	x	1.64
32 CTSB	1.00	0.00	0.00	1.00	0.00	0.00	0.00	1.00	0.00	1.00	0.00	0.00	x	x	x	x	5.36	x
33 CYBSR1	1.00	0.00	0.00	1.00	0.00	0.00	0.00	1.00	0.00	1.00	0.00	0.00	x	x	x	x	5.62	x
34 DACHI	1.00	0.00	0.00	1.00	0.00	0.00	0.00	1.00	0.00	0.00	1.00	0.00	x	x	x	x	x	1.53
35 DDIT3	1.00	0.00	0.00	1.00	0.00	0.00	0.00	1.00	0.00	1.00	0.00	0.00	x	x	x	x	0.1	x
36 DPYSL5	1.00	0.00	0.00	1.00	0.00	0.00	0.00	1.00	0.00	1.00	0.00	0.00	x	x	x	x	2.77	x
37 DUSP1	0.22	0.10	0.68	1.00	0.00	0.00	0.00	1.00	0.00	1.00	0.00	0.00	1.18	0.09	x	x	6.12	x
38 EDIL3	1.00	0.00	0.00	1.00	0.00	0.00	1.00	0.00	0.00	0.43	0.47	0.10	x	x	x	x	x	0.69
39 EFEMP1	1.00	0.00	0.00	1.00	0.00	0.00	0.00	1.00	0.00	1.00	0.00	0.00	x	x	x	x	2.09	x
40 ENPP2	1.00	0.00	0.00	1.00	0.00	0.00	0.00	1.00	0.00	1.00	0.00	0.00	x	x	x	x	17.02	x
41 EVL	1.00	0.00	0.00	1.00	0.00	0.00	0.00	1.00	0.00	1.00	0.00	0.00	x	x	x	x	0.17	x
42 FAM98A	1.00	0.00	0.00	1.00	0.00	0.00	0.00	1.00	0.00	1.00	0.00	0.00	x	x	x	x	3.85	x
43 FBXL17	1.00	0.00	0.00	1.00	0.00	0.00	0.00	1.00	0.00	1.00	0.00	0.00	x	x	x	x	5.43	x
44 FGD4	0.00	1.00	0.00	1.00	0.00	0.00	0.00	1.00	0.00	1.00	0.00	0.00	1.13	0.06	x	x	x	x
45 FMNL3	1.00	0.00	0.00	1.00	0.00	0.00	0.00	1.00	0.00	1.00	0.00	0.00	x	x	x	x	0.06	x
46 FNDC3A	1.00	0.00	0.00	1.00	0.00	0.00	0.00	1.00	0.00	1.00	0.00	0.00	x	x	x	x	5.18	x
47 FOCAD	1.00	0.00	0.00	1.00	0.00	0.00	0.00	1.00	0.00	1.00	0.00	0.00	x	x	x	x	x	0.7
48 FRAS1	1.00	0.00	0.00	1.00	0.00	0.00	0.00	1.00	0.00	1.00	0.00	0.00	x	x	x	x	4.4	x
49 FSD1	1.00	0.00	0.00	1.00	0.00	0.00	0.00	1.00	0.00	1.00	0.00	0.00	x	x	x	x	2.13	x
50 FSTL5	1.00	0.00	0.00	1.00	0.00	0.00	0.00	1.00	0.00	1.00	0.00	0.00	x	x	x	x	x	0.71
51 GABARAPL1	0.49	0.38	0.13	1.00	0.00	0.00	1.00	0.00	0.00	1.00	0.00	0.00	1.11	0.04	x	x	x	x
52 GABRG3	1.00	0.00	0.00	1.00	0.00	0.00	0.00	1.00	0.00	1.00	0.00	0.00	x	x	x	x	4.58	x
53 GALNT13	1.00	0.00	0.00	1.00	0.00	0.00	0.00	1.00	0.00	0.00	1.00	0.00	x	x	x	x	x	0.7
54 GLIS3	1.00	0.00	0.00	1.00	0.00	0.00	0.00	1.00	0.00	0.00	1.00	0.00	x	x	x	x	x	1.53
55 GPR183	1.00	0.00	0.00	1.00	0.00	0.00	0.00	1.00	0.00	1.00	0.00	0.00	x	x	x	x	0.02	x
56 GRIA2	1.00	0.00	0.00	1.00	0.00	0.00	0.00	1.00	0.00	1.00	0.00	0.00	x	x	x	x	2.08	x
57 HAGH	1.00	0.00	0.00	1.00	0.00	0.00	0.00	1.00	0.00	1.00	0.00	0.00	x	x	x	x	0.15	x

Continued on next page

Gene	P^{null} RNA local	P^{ben} RNA local	P^{del} RNA local	P^{null} RNA piMOM	P^{ben} RNA piMOM	P^{del} RNA piMOM	P^{null} GWAS local	P^{ben} GWAS local	P^{del} GWAS local	P^{null} GWAS piMOM	P^{ben} GWAS piMOM	P^{del} GWAS piMOM	RNA effect local	Dispersion local	RNA effect piMOM	Dispersion piMOM	GWAS effect local	GWAS effect piMOM
58 HAPI	1.00	0.00	0.00	1.00	0.00	0.00	0.00	1.00	0.00	1.00	0.00	0.00	x	x	x	x	4.58	x
59 HDAC9	1.00	0.00	0.00	1.00	0.00	0.00	1.00	0.00	0.00	0.14	0.81	0.05	x	x	x	x	x	0.74
60 HLA-DPA1	1.00	0.00	0.00	1.00	0.00	0.00	0.00	0.00	1.00	1.00	0.00	0.00	x	x	x	x	4.21	x
61 HSPA2	1.00	0.00	0.00	1.00	0.00	0.00	0.00	0.00	1.00	1.00	0.00	0.00	x	x	x	x	33.82	x
62 HSPA6	1.00	0.00	0.00	1.00	0.00	0.00	1.00	0.00	0.00	0.00	0.00	1.00	x	x	x	x	x	0.6
63 IDH3A	1.00	0.00	0.00	1.00	0.00	0.00	0.00	0.00	1.00	1.00	0.00	0.00	x	x	x	x	0.22	x
64 IFRD1	0.00	1.00	0.00	1.00	0.00	0.00	1.00	0.00	0.00	1.00	0.00	0.00	1.13	0.07	x	x	x	x
65 IQCA1	1.00	0.00	0.00	1.00	0.00	0.00	0.00	0.00	1.00	1.00	0.00	0.00	x	x	x	x	2.34	x
66 JPH4	1.00	0.00	0.00	1.00	0.00	0.00	0.00	0.00	1.00	1.00	0.00	0.00	x	x	x	x	0.01	x
67 KATNB1	1.00	0.00	0.00	1.00	0.00	0.00	0.00	0.00	1.00	1.00	0.00	0.00	x	x	x	x	3.68	x
68 KBTBD8	1.00	0.00	0.00	1.00	0.00	0.00	0.00	0.00	1.00	1.00	0.00	0.00	x	x	x	x	1.59	x
69 KCNJ6	1.00	0.00	0.00	1.00	0.00	0.00	0.00	0.00	1.00	1.00	0.00	0.00	x	x	x	x	3.6	x
70 KHDC1	1.00	0.00	0.00	1.00	0.00	0.00	0.00	0.00	1.00	1.00	0.00	0.00	x	x	x	x	6.61	x
71 KHDRBS3	1.00	0.00	0.00	1.00	0.00	0.00	0.00	0.00	1.00	1.00	0.00	0.00	x	x	x	x	3.33	x
72 KLK6	1.00	0.00	0.00	1.00	0.00	0.00	0.00	0.00	1.00	1.00	0.00	0.00	x	x	x	x	44.74	x
73 LAPTM5	1.00	0.00	0.00	1.00	0.00	0.00	0.00	0.00	1.00	1.00	0.00	0.00	x	x	x	x	2.14	x
74 LINC01197	1.00	0.00	0.00	1.00	0.00	0.00	0.00	0.00	1.00	1.00	0.00	0.00	x	x	x	x	0.45	x
75 LPAR6	1.00	0.00	0.00	1.00	0.00	0.00	0.00	0.00	1.00	1.00	0.00	0.00	x	x	x	x	0.13	x
76 LRRN1	1.00	0.00	0.00	1.00	0.00	0.00	0.00	0.00	1.00	1.00	0.00	0.00	x	x	x	x	3.8	x
77 MAP4K5	1.00	0.00	0.00	1.00	0.00	0.00	0.00	0.00	1.00	1.00	0.00	0.00	x	x	x	x	1.7	x
78 MARCKSL1	1.00	0.00	0.00	1.00	0.00	0.00	0.00	0.00	1.00	1.00	0.00	0.00	x	x	x	x	0.04	x
79 MAST2	1.00	0.00	0.00	1.00	0.00	0.00	1.00	0.00	0.00	0.00	0.00	1.00	x	x	x	x	x	0.68
80 MFSD4A	1.00	0.00	0.00	1.00	0.00	0.00	0.00	0.00	1.00	1.00	0.00	0.00	x	x	x	x	0.25	x
81 MOCS2	1.00	0.00	0.00	1.00	0.00	0.00	0.00	0.00	1.00	1.00	0.00	0.00	x	x	x	x	2.6	x
82 MRPL55	1.00	0.00	0.00	1.00	0.00	0.00	0.00	0.00	1.00	1.00	0.00	0.00	x	x	x	x	25.93	x
83 NCALD	1.00	0.00	0.00	1.00	0.00	0.00	0.00	0.00	1.00	1.00	0.00	0.00	x	x	x	x	0.42	x
84 NKAIN2	1.00	0.00	0.00	1.00	0.00	0.00	0.00	0.00	1.00	1.00	0.00	0.00	x	x	x	x	6.08	x
85 NSF	1.00	0.00	0.00	1.00	0.00	0.00	0.00	0.00	1.00	1.00	0.00	0.00	x	x	x	x	0.48	x
86 NUTF2	1.00	0.00	0.00	1.00	0.00	0.00	0.00	0.00	1.00	1.00	0.00	0.00	x	x	x	x	4.29	x
87 ORMDL1	1.00	0.00	0.00	1.00	0.00	0.00	0.00	0.00	1.00	1.00	0.00	0.00	x	x	x	x	55.44	x

Continued on next page

Gene	P^{null} RNA local	P^{ben} RNA local	P^{del} RNA local	P^{null} RNA piMOM	P^{ben} RNA piMOM	P^{del} RNA piMOM	P^{null} GWAS local	P^{ben} GWAS local	P^{del} GWAS local	P^{null} GWAS piMOM	P^{ben} GWAS piMOM	P^{del} GWAS piMOM	RNA effect local	Dispersion local	RNA effect piMOM	Dispersion piMOM	GWAS effect local	GWAS effect piMOM
88 PACSINI	1.00	0.00	0.00	1.00	0.00	0.00	1.00	0.00	1.00	1.00	0.00	0.00	x	x	x	x	3.01	x
89 PCSK5	1.00	0.00	0.00	1.00	0.00	0.00	1.00	0.00	0.00	0.00	1.00	0.00	x	x	x	x	x	2.22
90 PELI1	0.12	0.83	0.05	1.00	0.00	0.00	1.00	0.00	0.00	1.00	0.00	0.00	1.11	0.05	x	x	x	x
91 PGAMI	1.00	0.00	0.00	1.00	0.00	0.00	1.00	0.00	1.00	1.00	0.00	0.00	x	x	x	x	68.49	x
92 PLEKHB1	1.00	0.00	0.00	1.00	0.00	0.00	1.00	0.00	1.00	1.00	0.00	0.00	x	x	x	x	2.32	x
93 PLEKHB2	1.00	0.00	0.00	1.00	0.00	0.00	1.00	0.00	1.00	1.00	0.00	0.00	x	x	x	x	30.29	x
94 PTPRD	1.00	0.00	0.00	1.00	0.00	0.00	1.00	0.00	1.00	1.00	0.00	0.00	x	x	x	x	x	1.49
95 PTPRG	1.00	0.00	0.00	1.00	0.00	0.00	1.00	0.00	1.00	1.00	0.00	0.00	x	x	x	x	x	2.18
96 PTPRR	1.00	0.00	0.00	1.00	0.00	0.00	1.00	0.00	1.00	1.00	0.00	0.00	x	x	x	x	1.56	x
97 RAMP1	1.00	0.00	0.00	1.00	0.00	0.00	1.00	0.00	1.00	1.00	0.00	0.00	x	x	x	x	35.86	x
98 RANBP2	1.00	0.00	0.00	1.00	0.00	0.00	1.00	0.00	1.00	1.00	0.00	0.00	x	x	x	x	0.27	x
99 RAPIGAP	0.22	0.10	0.68	1.00	0.83	0.02	1.00	0.00	1.00	1.00	0.00	0.00	0.58	1.5	0.6	1.49	x	x
100 RHOQ	1.00	0.00	0.00	1.00	0.00	0.00	1.00	0.00	1.00	1.00	0.00	0.00	x	x	x	x	8.8	x
101 S100B	1.00	0.00	0.00	1.00	0.00	0.00	1.00	0.00	1.00	1.00	0.00	0.00	x	x	x	x	0.47	x
102 SCN1A	1.00	0.00	0.00	1.00	0.00	0.00	1.00	0.00	1.00	1.00	0.00	0.00	x	x	x	x	2.85	x
103 SCRIN2	1.00	0.00	0.00	1.00	0.00	0.00	1.00	0.00	1.00	1.00	0.00	0.00	x	x	x	x	2.57	x
104 SEMA3B	1.00	0.00	0.00	1.00	0.00	0.00	1.00	0.00	1.00	1.00	0.00	0.00	x	x	x	x	8.22	x
105 SERINC3	1.00	0.00	0.00	1.00	0.00	0.00	1.00	0.00	1.00	1.00	0.00	0.00	x	x	x	x	0.1	x
106 SLC24A2	1.00	0.00	0.00	1.00	0.00	0.00	1.00	0.00	1.00	1.00	0.00	0.00	x	x	x	x	x	0.67
107 SLC25A29	1.00	0.00	0.00	1.00	0.00	0.00	1.00	0.00	1.00	1.00	0.00	0.00	x	x	x	x	0.03	x
108 SYT13	1.00	0.00	0.00	1.00	0.00	0.00	1.00	0.00	1.00	1.00	0.00	0.00	x	x	x	x	2.34	x
109 SYT5	1.00	0.00	0.00	1.00	0.00	0.00	1.00	0.00	1.00	1.00	0.00	0.00	x	x	x	x	25.12	x
110 TIMM22	1.00	0.00	0.00	1.00	0.00	0.00	1.00	0.00	1.00	1.00	0.00	0.00	x	x	x	x	69.37	x
111 TLR6	1.00	0.00	0.00	1.00	0.00	0.00	1.00	0.00	1.00	1.00	0.00	0.00	x	x	x	x	4.82	x
112 TMEM125	1.00	0.00	0.00	1.00	0.00	0.00	1.00	0.00	1.00	1.00	0.00	0.00	x	x	x	x	0.17	x
113 TMEM181	1.00	0.00	0.00	1.00	0.00	0.00	1.00	0.00	1.00	1.00	0.00	0.00	x	x	x	x	0.17	x
114 TMEM246	1.00	0.00	0.00	1.00	0.00	0.00	1.00	0.00	1.00	1.00	0.00	0.00	x	x	x	x	0.54	x
115 TMTC1	1.00	0.00	0.00	1.00	0.00	0.00	1.00	0.00	1.00	1.00	0.00	0.00	x	x	x	x	x	1.33
116 TPI1	1.00	0.00	0.00	1.00	0.00	0.00	1.00	0.00	1.00	1.00	0.00	0.00	x	x	x	x	15.83	x
117 TRPS1	1.00	0.00	0.00	1.00	0.00	0.00	1.00	0.00	1.00	1.00	0.00	0.00	x	x	x	x	3.56	x

Continued on next page

Gene	P^{null} RNA local	P^{ben} RNA local	P^{del} RNA local	P^{null} RNA piMOM	P^{ben} RNA piMOM	P^{del} RNA piMOM	P^{null} GWAS local	P^{ben} GWAS local	P^{del} GWAS local	P^{null} GWAS piMOM	P^{ben} GWAS piMOM	P^{del} GWAS piMOM	RNA effect local	Dispersion local	RNA effect piMOM	Dispersion piMOM	GWAS effect local	GWAS effect piMOM
118 TUFM	1.00	0.00	0.00	1.00	0.00	0.00	0.00	0.00	1.00	1.00	0.00	0.00	x	x	x	x	25.96	x
119 UQCR10	1.00	0.00	0.00	1.00	0.00	0.00	0.00	1.00	0.00	1.00	0.00	0.00	x	x	x	x	2.07	x
120 UQCRC1	1.00	0.00	0.00	1.00	0.00	0.00	0.00	0.00	1.00	1.00	0.00	0.00	x	x	x	x	0.39	x
121 WDR12	1.00	0.00	0.00	1.00	0.00	0.00	0.00	0.00	1.00	1.00	0.00	0.00	x	x	x	x	1.77	x
122 XYLT1	1.00	0.00	0.00	1.00	0.00	0.00	1.00	0.00	0.00	0.00	1.00	0.00	x	x	x	x	x	1.36
123 ZDHHC20	1.00	0.00	0.00	1.00	0.00	0.00	0.00	0.00	1.00	1.00	0.00	0.00	x	x	x	x	0.22	x

Table 4: Genes identified as non-null in either the TG RNA only model or GWAS only model with proportion of time spent in each group and effect sizes as in Manuscript Table 1. The top 94 genes in the GWAS only local model are reported (a cutoff of 0.9999) as opposed to all genes in the median model which is used for the other three models.